DESIGN OF APERTURE COUPLED DUAL BAND MICROSTRIP RECTANGULAR PATCH ANTENNA FOR WLAN AND PCS APPLICATIONS

A Thesis submitted in partial fulfillment of the

Requirements for the award of the Degree of

MASTER OF ENGINEERING

IN

ELECTRONICS AND COMMUNICATION ENGINEERING

Submitted By:-

Ved Prakash

Roll No. 800961020

Under the guidance of:-

Dr. Rajesh Khanna

Professor, ECED

Thapar University, Patiala

DEPARTMENT OF ELECTRONICS AND COMMUNICATION ENGINEERING,

THAPAR UNIVERSITY

PATIALA-147001, PUNJAB, INDIA

JUNE, 2011

CERTIFICATE

I, Ved Prakash hereby certify that the work which is being presented in this thesis entitled **"Design of Aperture Coupled Dual Band Microstrip Rectangular Patch Antenna for WLAN and PCS Applications"** by me in partial fulfillment of the requirements for the award of degree of Masters of Engineering in Electronics and Communication Engineering from Thapar University, Patiala is an authentic record of my own work carried under the supervision of Dr. Rajesh Khanna and referred other researcher's work which are duly listed in the reference section.

The matter presented in this report has not been submitted in any University/Institute for the award of Masters of Engineering.

Ved Prakash

(Ved Prakash)

Date 24/06/2011

This is certified that the above statement made by the candidate is correct to best of my knowledge.

(Dr. Rajesh Khanna)

(Supervisor)

Date 24/6/11

Head of Department

Date 24/6/11

ECED, T.U. Patiala

(Dr. S.K. Mohapatra)

Dean of Academic Affairs

Date

T.U. Patiala

Abstract

Microstrip patch antennas (MPA) are well suited for integration into many applications owing to their conformal nature. There are many feeding techniques used for the Microstrip patch antennas. Feeding technique such as coaxial feed (probe feed) has disadvantages like drilling a hole in substrate and protruding connector due to which the antenna structure is not completely planar. Also, this feeding arrangement makes the configuration asymmetrical. To keep the structure planar, a microstrip line in the plane of the patch can be etched to feed the antenna. But again, it suffers from the drawbacks that the feed network interferes with the radiating properties of the antenna leading to undesired radiations. Also, for thick substrates, which are generally employed to achieve broad Bandwidth, both the feeding methods discussed above of direct feeding the Microstrip patch antennas have some problems. In the case of a coaxial feed, increased probe length makes the input impedance more inductive, leading to the matching problem. For the microstrip feed, an increase in the substrate thickness increases its width, which in turn increases the undesired feed radiations.

So the coupling techniques with the feed lines in the plane other then the antenna are more suitable. Aperture coupled feed and proximity feed are two such feed techniques. Of these, aperture coupled feed increases the bandwidth of the antenna and is the most convenient feeding technique. Apart from this, aperture coupling provides a greater radiation pattern symmetry and greater ease of design for higher impedance bandwidth owing to a large number of design parameters. In this type of feed, by using multiple patches bandwidth up to 70% are reported (however only single patch design is attempted in this thesis). Also, the multilayered substrates need to be properly aligned.

So in this thesis, an aperture coupled antenna resonating at 2.43GHz, providing 144 MHz bandwidth for WLAN application is designed in CST MICROWAVE STUDIO 9. Loading slots at the non-resonating sides of the patch of single band aperture coupled antenna make it dual band for WLAN (2.40-2.48 GHz) and personal communication system (2.18-2.20 GHz).

The parametric study of the designed antenna and its fabrication has been attempted in this thesis. The physical parameters examined in this study include the

dimensions and locations of the substrates and their dielectric constants, feed line, ground plane coupling slot, and patch. The antenna parameters like operating frequency, input impedance, VSWR, Bandwidth, Return loss, directivity and gain are determined for each antenna configuration.

The operating frequency, input impedance, VSWR, Bandwidth, Return loss, directivity and gain of the single band antenna designed are 2.43GHz, 75ohm, 1.0325, 142MHz, -29.923dB, 5.372 dBi and 6.167 dB respectively. The percentage bandwidth of the antenna is 5.84.The dual band antenna having two slots on the non-resonating sides of patch resonates at 2.20 GHz and 2.45 GHz and provides a percentage bandwidth of 2.27 and 3.67 respectively. The directivity of the antenna at 2.20GHz and 2.45 GHz are 5.033dBi and 5.402dBi, and gain is 5.849 dB and 6.0229dB respectively.

ACKNOWLEDGEMENT

This thesis is completed with prayer of many and love of my family and friends. However, there are few people that I would like to specially acknowledge and extend my heartfelt gratitude who have made the completion of this thesis possible. With the biggest contribution to this thesis; I would like to thank **Dr. Rajesh Khanna** had given me his full support in guiding me with stimulating suggestions and encouragement to go ahead in all the time of the thesis.

I am also thankful to **Dr. A. K. Chatterjee,** Head, Electronics and Communication Engineering Department, for providing us with the adequate infrastructure in carrying the work.

I am also thankful to **Dr. Alpana Agarwal**, P.G. Coordinator, Electronics and Communication Engineering department, for the motivation and inspiration that triggered me for the thesis.

At last but not the least my gratitude towards my parents and relatives, I would also like to thank God for not letting me down at a time of crisis and showing me the silver lining in the dark clouds.

Ved Prakash
(800961020)

Table of Contents

List of Figures

List of Tables

Abbreviations

MPA	Microstrip Patch Antenna
ACRPMA	Aperture coupled rectangular patch microstrip antenna
FDTD	Finite-difference time-domain
WLAN	Wireless local area network
PCS	Personal communication system
Q	Quality factor
CST	Computer Simulation Technology
NUFFT	Non-uniform fast Fourier transform
VSWR	Voltage standing wave ratio

CHAPTER 1

An Overview of Microstrip Patch Antenna

In this chapter, an introduction to the Microstrip Patch Antenna (MPA) is given, followed by its advantages and disadvantages. Some feed modeling techniques are also discussed. The overview of FDTD analysis technique and designing an antenna is also given. It covers the electromagnetic spectrum used for the various applications.

1.1Introduction

In its most basic form, a Microstrip patch antenna consists of a radiating patch on one side of a dielectric substrate which has a ground plane on the other side as shown in Figure 1.1. The patch is generally made of conducting material such as copper or gold and can take any possible shape. The radiating patch and the feed lines are usually photo etched on the dielectric substrate.

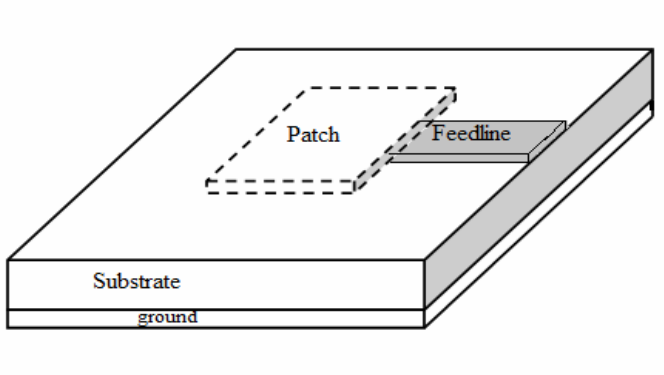

Figure 1.1 Structure of a Microstrip Patch Antenna

For a rectangular patch, the length L of the patch is usually $0.3333\,\lambda_o < L < 0.5\lambda_o$, where λ_o is the free-space wavelength. The patch is selected to be very thin such that $t << \lambda_o$ (where t is the patch thickness). The height h of the dielectric substrate is usually $0.003\,\lambda_o \leq h \leq 0.05\,\lambda_o$. The dielectric constant of the substrate (ε_r) is typically in the range $2.2 \leq \varepsilon_r \leq 12$.

Microstrip patch antennas radiate primarily because of the fringing fields between the patch edge and the ground plane. For good antenna performance, a thick dielectric substrate having a low dielectric constant is desirable since this provides better efficiency, larger bandwidth and better radiation[2], [5]. However, such a configuration leads to a larger antenna size. In order to design a compact Microstrip patch antenna, higher dielectric constants must be used which are less efficient and

result in narrower bandwidth. Hence a compromise must be reached between antenna dimensions and antenna performance.

1.2 Advantages and Disadvantages

Microstrip patch antennas are increasing in popularity for use in wireless applications due to their low-profile structure. Therefore they are extremely compatible for embedded antennas in handheld wireless devices such as cellular phones, pagers etc. The telemetry and communication antennas on missiles need to be thin and conformal and are often Microstrip patch antennas. Another area where they have been used successfully is in Satellite communication. Some of their principal advantages are given below [5]:

- Light weight and low volume.
- Low profile planar configuration which can be easily made conformal to host surface.
- Low fabrication cost, hence can be manufactured in large quantities.
- Supports both, linear as well as circular polarization.
- Can be easily integrated with microwave integrated circuits (MICs).
- Capable of dual and triple frequency operations.
- Mechanically robust when mounted on rigid surfaces

Microstrip patch antennas suffer from a number of disadvantages as compared to conventional antennas. Their major disadvantages are [5]

- Narrow bandwidth.
- Low efficiency.
- Low Gain.
- Extraneous radiation from feeds and junctions.
- Poor end fire radiator except tapered slot antennas.
- Low power handling capacity.
- Surface wave excitation.

Microstrip patch antennas have a very high antenna quality factor (Q). Q represents the losses associated with the antenna and a large Q leads to narrow bandwidth and low efficiency. Q can be reduced by increasing the thickness of the dielectric substrate. But as the thickness increases, an increasing fraction of the total power delivered by the source goes into a surface wave. This surface wave contribution can be counted as an unwanted power loss since it is ultimately scattered at the dielectric

bends and causes degradation of the antenna characteristics. However, surface waves can be minimized by use of photonic band gap structures [2]. Other problems such as lower gain and lower power handling capacity can be overcome by using an array configuration for the elements.

1.3 Feeding techniques

Microstrip patch antennas can be fed by a variety of methods. These methods can be classified into two categories- contacting and non-contacting. In the contacting method, the RF power is fed directly to the radiating patch using a connecting element such as a microstrip line. In the non-contacting scheme, electromagnetic field coupling is done to transfer power between the microstrip line and the radiating patch. The four most popular feed techniques used are the microstrip line, coaxial probe (both contacting schemes), aperture coupling and proximity coupling (both non-contacting schemes)[2]-[7].

A **microstrip feed** uses a transmission line to connect the radiating patch to receive or transmit circuitry. Electromagnetic field lines are focused between the microstrip line and ground plane to excite only guided waves as opposed to radiated or surface waves. Guided waves dominate in electrically thin dielectrics with relatively large permittivities [2]. For the patch antenna, radiated waves at the patch edges are maximized using electrically thick dielectric substrates with relatively low permittivities. Hence, it is difficult to meet substrate height and permittivity requirements for both the microstrip transmission line and patch antenna. Dielectric substrates selected to satisfy the two conflicting criteria increase surface waves, reduce radiation efficiency due to increased guided waves below the patch, and increase side-lobes and cross-polarization levels from spurious feed line radiation [2]. A microstrip line feed is generally used in two configurations namely Directly fed and Inset feed as shown in the figure 1.2.

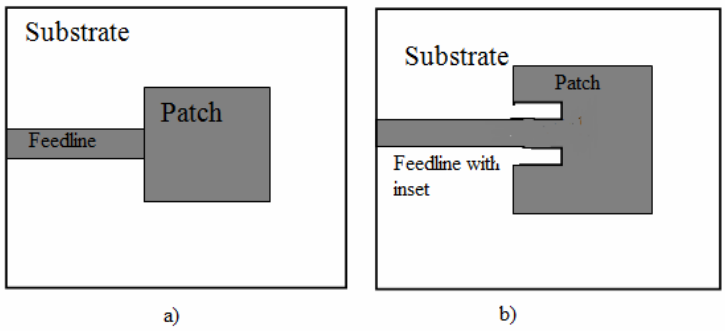

Figure 1.2: Geometry of microstrip line feed (a) directly feed and (b) Inset feed

A **probe fed** antenna consists of a microstrip patch fed by the center conductor of a coaxial line (see Figure 1.3). The outer coax conductor is electrically connected to the ground plane. Due to the absence of a microstrip feed line, the substrate thickness and permittivity can be designed to maximize antenna radiation. However, the probe center conductor underneath the patch causes undesired distortion in the electric field between the patch and ground plane and produces undesired reactive loading effects at the antenna input port [2], [3]. The undesired reactance can be compensated by adjusting the probe location on the patch.

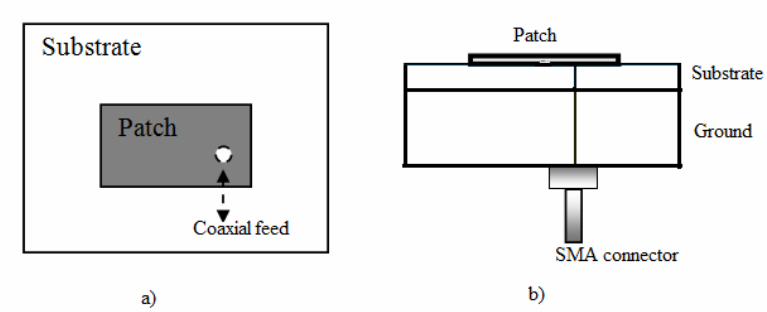

Figure 1.3: Geometry of coaxial probe feed microstrip patch antenna (a) top view and (b) side view.

In **Aperture Coupled** feeding technique, the radiating patch and the microstrip feedline are separated by the ground plane thereby eliminating the direct electrical connection between the conducting feed and radiating patch (see figure 1.4). Coupling between the patch and the feed line is made through a slot or an aperture in the ground plane.

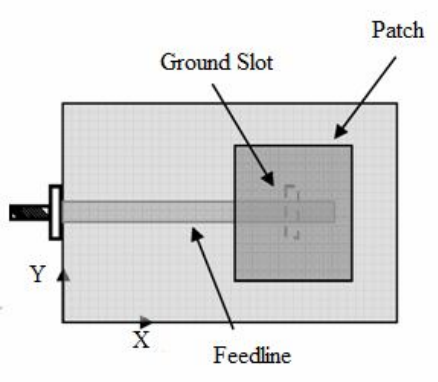

Figure1.4: Geometry of an aperture coupled feed microstrip patch antenna (top view).

The coupling aperture is usually centered under the patch, leading to lower cross-polarization due to symmetry of the configuration. The amount of coupling from the feed line to the patch is determined by the shape, size and location of the aperture. Since the ground plane separates the patch and the feed line, spurious radiation is minimized. Generally, a high dielectric material is used for the bottom substrate and a thick, low dielectric constant material is used for the top substrate to optimize radiation from the patch [5]. Aperture coupled antennas are advantageous in arrays because they electrically isolate the feed and phase shifting circuitry from the patch antennas. The disadvantage is the required multilayer structure which increases fabrication complexity and cost [2]. The major disadvantage of this feed technique is that it is difficult to fabricate due to multiple layers, which also increases the antenna thickness. This feeding scheme also provides narrow bandwidth.

The **Proximity Coupled Feed** technique is also called as the electromagnetic coupling scheme. As shown in Figure 1.5, two dielectric substrates are used such that the feed line is between the two substrates and the radiating patch is on top of the upper substrate. The main advantage of this feed technique is that it eliminates spurious feed radiation and provides very high bandwidth (as high as 13%) [5], due to overall increase in the thickness of the microstrip patch antenna. This scheme also provides choices between two different dielectric media, one for the patch and one for the feed line to optimize the individual performances. Matching can be achieved by controlling the length of the feed line and the width-to-line ratio of the patch. The major disadvantage of this feed scheme is that it is difficult to fabricate because of the two dielectric layers which need proper alignment. Also, there is an increase in the overall thickness of the antenna.

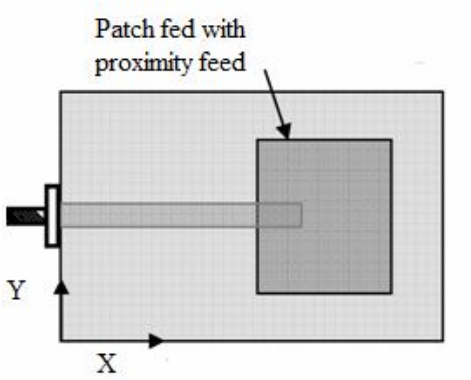

Figure 1.5: Geometry of a proximity coupled microstrip feed microstrip patch antenna (top view)

The comparison of the feeding techniques in tabulated form is given by table 1.1

Table1.1: (The comparisons between the feeding methods for microstrip patch antenna)

Feeding technique	Advantages	Disadvantages
Proximity Coupled	▪ No direct contact between feed and patch. ▪ Can have large effective thickness for patch substrate and much thinner feed substrate.	▪ Multilayer fabrication required.
Microstrip Line	▪ Monolithic ▪ Easy to fabricate. ▪ Easy to match by controlling Insert position.	▪ Spurious radiation from feed line, especially for thick substrate when line width is significant.
Coaxial Feed	▪ Easy to match. ▪ Low spurious radiation.	▪ Large inductance for thick substrate. ▪ Soldering required.

Aperture Coupled	▪ Use of two substrates avoids deleterious effect of a high-dielectric constant substrate on the bandwidth and efficiency. ▪ No direct contact between feed and patch avoiding large probe reactance or width microstrip line. ▪ No radiation from the feed and active devices since a ground plane separates them from the radiating patch	▪ Multilayer fabrication required. ▪ Higher back-lobe radiation.

1.4 Methods of Analysis

The various models for the analysis of Microstrip patch antennas are the transmission line model [3] [8]-[10], cavity model [11]-[13], FDTD [14]-[16] and full wave model [5].The transmission line model is the simplest of all and it gives good physical insight but it is less accurate. The cavity model is more accurate but is complex in nature. The full wave models are extremely accurate, versatile and can treat single elements and arrays. The FDTD method is easy to understand and implement in software. CST Microwave studio uses the FDTD scheme.

Finite-difference time-domain (FDTD) is a popular computational electrodynamics modeling technique. It is a time-domain method and solutions can cover a wide frequency range with a single simulation run. The basic FDTD space grid and time-stepping algorithm trace back to a seminal 1966 paper by Kane Yee [14].The descriptor "Finite-difference time-domain" and its corresponding "FDTD" acronym were originated by Allen Taflove [15]. The FDTD method belongs in the general class of *grid-based differential time-domain numerical modeling* methods. This method includes the following steps:

1) *Discretization of fields* using central-difference approximations to the space and time partial derivatives.

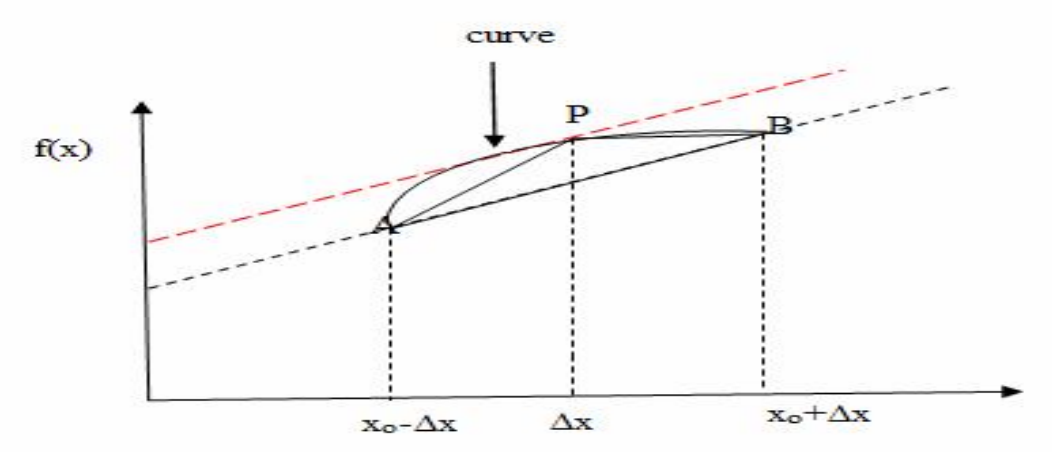

Figure 1.6: Differention of the curve APB [17].

Consider the figure 1.6 where a simple differentiation of a curve is shown in 2D. Using the central difference scheme, we have

$$f'(x_o) \approx \frac{f(x_o + \Delta x) - f(x_o - \Delta x)}{2\Delta x}$$

……(1.1)

Now, consider the Maxwell's equations as written below

$$\nabla \times \boldsymbol{H} = \frac{\partial \boldsymbol{D}}{\partial t} + \boldsymbol{J}$$ ……..(1.2)

$$\nabla \times \boldsymbol{E} = -\frac{\partial \boldsymbol{B}}{\partial t}$$ ……..(1.3)

$$\nabla . \boldsymbol{D} = 0$$ …… (1.4)

$$\nabla . \boldsymbol{B} = 0$$ ……(1.5)

and

$$\boldsymbol{D} = \varepsilon_o \varepsilon \boldsymbol{E}, \qquad \boldsymbol{B} = \mu_o \mu \boldsymbol{H}$$ ……. (1.6)

Consider 1D system where a wave is travelling in x-direction and **E**-field is along y axis and **H**-field is along z-axis.

$$\boldsymbol{E(r,t) \rightarrow E_y(x,t)}$$

$$\boldsymbol{H(r,t) \rightarrow H_z(x,t)}$$

Equations (1.2) and (1.3) can be written as

$$\frac{\partial H_Z}{\partial t} = -\frac{1}{\mu_o \mu}\frac{\partial E_y}{\partial x} \quad \text{.....} \quad (1.7)$$

$$\frac{\partial E_y}{\partial t} = -\frac{1}{\varepsilon_o \varepsilon}\frac{\partial H_z}{\partial x}$$

.....(1.8)

2) *Solving the finite-difference equations*

The resulting finite-difference equations are solved in either software or hardware in a leapfrog manner. Firstly, a general problem is discussed and then Maxwell's equations are solved. Consider a uniform grid x_i as shown in the figure 1.7

Uniform grid: $\{x_i\}$, $x_i = i\,h$, $i = 0,1,2,3,\ldots\ldots$and $u_i = u(x_i)$

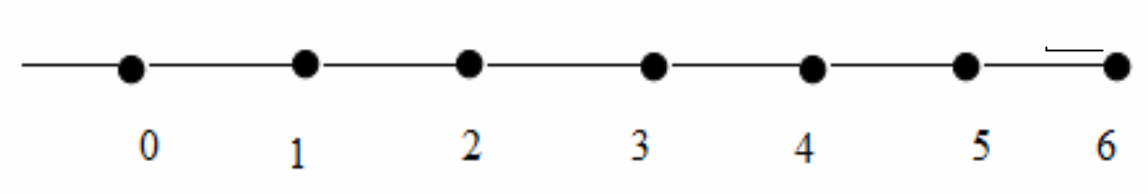

Figure 1.7: A uniform grid [18].

According to the Finite difference scheme, the partial differentiation of the u_i can be written as

$$\frac{du_i}{dx} = \frac{u_{i+1} - u_i}{h} + O(h) = D^+ u_i + O(h) \quad \text{.....} \quad (1.9)$$

$$\frac{du_i}{dx} = \frac{u_i - u_{i-1}}{h} + O(h) = D^- u_i + O(h)$$

……..(1.10)

$$\frac{du_i}{dx} = \frac{u_{i+1} - u_{i-1}}{2h} + O(2h)^2 = D^c u_i + O(2h)^2$$

……..(1.11)

where $O(h)$ = any initial value of u_i and *h* is the increment in the consecutive grid values.

$D^+, D^- and\ D^c$ are the change in the value of the grid from jumping one step ahead, back and two steps ahead respectively.

Now the grid is traced in staggering and leapfrogging manner as shown in the figure 1.8

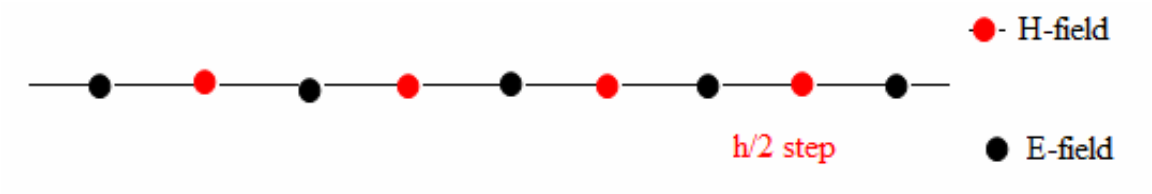

Figure 1.8: Staggering and leapfrogging of the grid [18].

Figure 1.9 shows the **E** and **H**-fields when the grid is staggering by h/2 step in space at time t = 0.

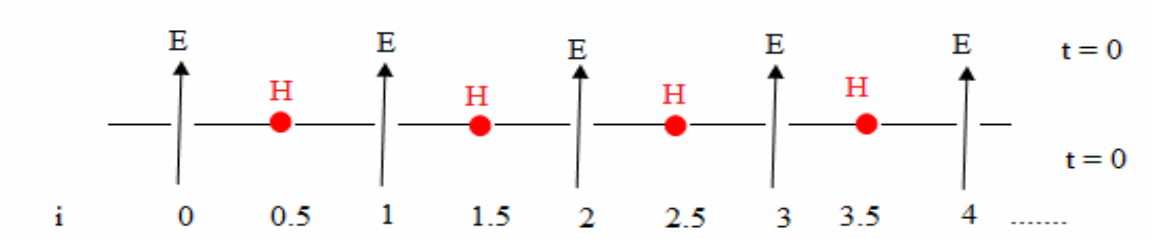

Figure 1.9: Staggering of grid by h/2 step[18].

3) *Solving the electric and magnetic field vector components* in a volume of space are solved subsequently at a given instant in time.

By replacing H_Z to H and E_y to E , the equations 1.7 and 1.8 are written as

$$\frac{\partial H}{\partial t} = -\frac{1}{\mu_o \mu} \frac{\partial E}{\partial x}$$ ……(1.12)

$$\frac{\partial E}{\partial t} = -\frac{1}{\varepsilon_o \varepsilon}\frac{\partial H}{\partial x} \quad \text{.....(1.13)}$$

When Maxwell's differential equations are examined, it can be seen that the change in the **E**-field in time (the time derivative) is dependent on the change in the **H**-field across space (the curl). This results in the basic FDTD time-stepping relation that, at any point in space, the updated value of the **E**-field in time is dependent on the stored value of the **E**-field and the numerical curl of the local distribution of the **H**-field in space [14].

Thus , for a particular grid at a given time,the equations 1.12 and 1.13 are written as

$$\frac{E_i^{n+1} - E_i^n}{\delta t} = -\frac{1}{\varepsilon_o \varepsilon_i}\frac{H_{i+1/2}^{n+1/2} - H_{i-1/2}^{n+1/2}}{\delta x} \quad \text{.....(1.14)}$$

$$\frac{H_{i+1/2}^{n+1/2} - H_{i+1/2}^{n-1/2}}{\delta t} = -\frac{1}{\mu_o \mu_{i+1/2}}\frac{E_{i+1}^n - E_i^n}{\delta x} \quad \text{.....(1.15)}$$

Figure 1.10 shows the view of the grids to calculate the **E** and **H** fields at cetain time periods.

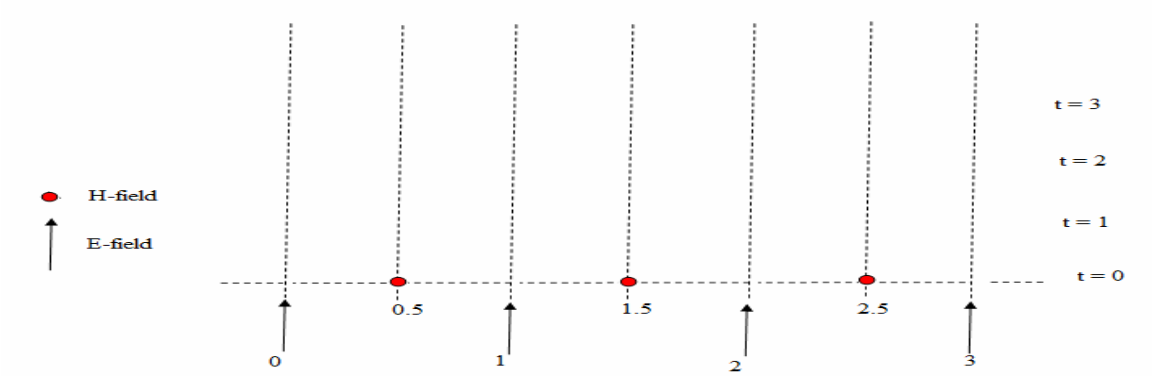

Figure 1.10: Calculation of E and H fields [18].

The normalized value of the **E**-field is given as

……(1.16)

The **H**-field is time-stepped in a similar manner as **E**-field. At any point in space, the updated value of the **H**-field in time is dependent on the stored value of the **H**-field and the numerical curl of the local distribution of the **E**-field in space. Iterating the **E**-field and **H**-field updates results in a marching-in-time process where in sampled-data analogs of the continuous electromagnetic waves under consideration propagate in a numerical grid stored in the computer memory.

Using the equations 1.16, 1.14 and 1.15 can be written as

$$H_{i+1/2}^{n+1/2} = H_{i+1/2}^{n-1/2} - \frac{Q}{\mu_{i+1/2}}\left(\widetilde{E_{i+1}^{n}} - \widetilde{E_{i}^{n}}\right) \quad \text{……(1.17)}$$

$$\widetilde{E_{i}^{n+1}} = \widetilde{E_{i}^{n}} - \frac{Q}{\varepsilon_i}\left(H_{i+1/2}^{n+1/2} - H_{i-1/2}^{n+1/2}\right) \quad \text{……...(1.18)}$$

where $Q = \dfrac{\delta t}{\sqrt{\varepsilon_o \mu_o}\,\delta x}$

Equation 1.18 in another form can be written as

$$\widetilde{E_{i}^{n+1}} = \widetilde{E_{i}^{n}} - \frac{Q}{\varepsilon_i}\left(H_{i+1/2}^{n+1/2} - H_{i-1/2}^{n+1/2}\right) \xrightarrow{-\delta x/2,\ -\delta t/2} \widetilde{E_{i}^{n+1}} = \widetilde{E_{i}^{n}} - \frac{Q}{\varepsilon_i}\left(H_{i}^{n} - H_{i-1}^{n}\right)$$

……...(1.19)

The figure 1.11 shows the genarilised method of computing the **E** and **H** fields.

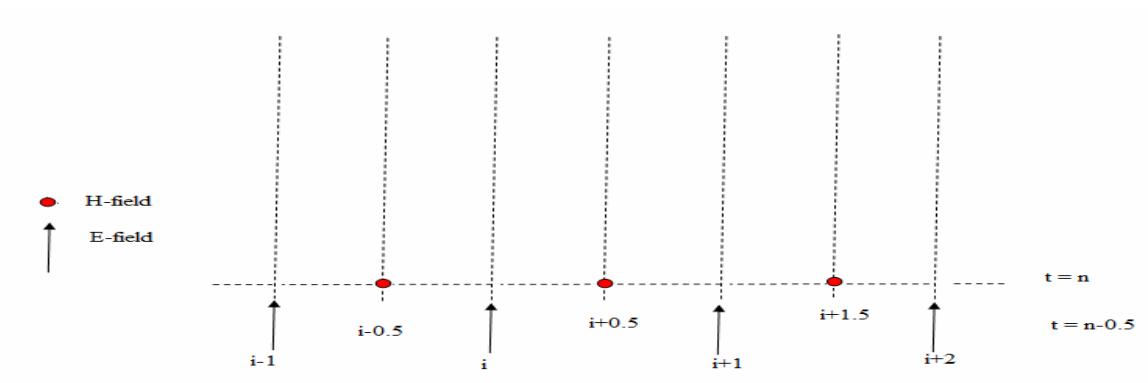

Figure 1.11: Genarilised method of computing the **E** and **H** fields[18].

$$\tilde{E}_i^{n+1} = \tilde{E}_i^{n} - \frac{Q}{\varepsilon_i}(H_i^n - H_{i-1}^n) \quad \text{(1.20)}$$

$$H_i^n = H_i^{n-1} - \frac{Q}{\mu_i}(\tilde{E}_{i+1}^{n} - \tilde{E}_i^{n}) \quad \text{(1.21)}$$

$$H_i^{n+1} = H_i^n - \frac{Q}{\mu_i}(\tilde{E}_{i+1}^{n+1} - \tilde{E}_i^{n+1}) \quad \text{(1.22)}$$

$$\frac{\partial E}{\partial x} \cong D_x^+ E \qquad \frac{\partial H}{\partial x} \cong D_x^- H \quad \text{(1.23)}$$

$$\frac{\partial E}{\partial t} \cong D_t^+ E \qquad \frac{\partial H}{\partial t} \cong D_t^- H \quad \text{(1.24)}$$

Thus, the equations 1.20 to 1.24 are solved for every interval. The process is repeated over and over again until the desired transient or steady-state electromagnetic field behavior is fully evolved.

Kane Yee's seminal 1966 paper proposed spatially staggering the vector components of the **E**-field and **H**-field about rectangular unit cells of a Cartesian computational grid so that each **E**-field vector component is located midway between a pair of **H**-field vector components, and conversely [14]. This scheme, now known as a Yee lattice, has proven to be very robust, and remains at the core of many current FDTD software constructs. Figure 1.12 shows the simple cubic unit cells of a grid.

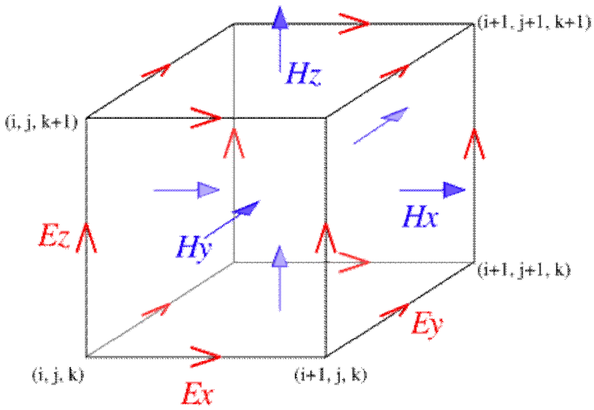

Figure 1.12: Grid structure of the fields (Yee lattice) [17]

In order to use FDTD a computational domain must be established. The computational domain is simply the physical region over which the simulation will be performed. The **E** and **H** fields are determined at every point in space within that computational domain. The material of each cell within the computational domain must be specified. Typically, the material is either free-space (air), metal, or dielectric. Any material can be used as long as the permeability, permittivity, and conductivity are specified.

Once the computational domain and the grid materials are established, a source is specified. The source can be an impinging plane wave, a current on a wire, or an applied electric field, depending on the application. Since the **E** and **H** fields are determined directly, the output of the simulation is usually the **E** or **H** field at a point or a series of points within the computational domain. The simulation evolves the **E** and **H** fields forward in time. Processing may be done on the **E** and **H** fields returned by the simulation. While the FDTD technique computes electromagnetic fields within a compact spatial region, scattered and/or radiated far fields can be obtained via near-to-far-field transformations.

1.5 General Comments on Designing Microstrip Patch Antennas

To design microstrip patch antennas meeting certain specifications, the antenna engineer should possess a combination of certain knowledge and skills. First, he/she should have an understanding of the principles of operation of the basic MPA structure. This can be obtained by studying the various modeling techniques like transmission line model, cavity model or FDTD etc.

According to the understanding and availability of the software, one can select and design the basic antenna structure in the software. Software can be selected from the Table 1.2.

Table 1.2(Software and their theoretical models)

Software Name	Theoretical model	Company Name
Ensemble	Moment method	Ansoft
IE3D	Moment method	Zeland
PCAAD	Cavity model	Antenna Design Associates
Fidelity	FDTD	Zeland

HFSS	Finite element	Ansoft
Microwave studio	FDTD	CST

The simulated results can be verified by mathematical modeling of antenna. But the mathematical analysis of the antenna becomes very complex for the structures having slots, shorted pins. The same antenna can also be designed in any other software for verification. But the best method to verify the results is to fabricate the antenna and get it tested to avail the measurement results. Here, in this thesis the CST Microwave Studio is used as the simulation tool which is based on the FDTD model of analysis. Figure 1.13 illustrates the design process of the antenna in form of a flowchart.

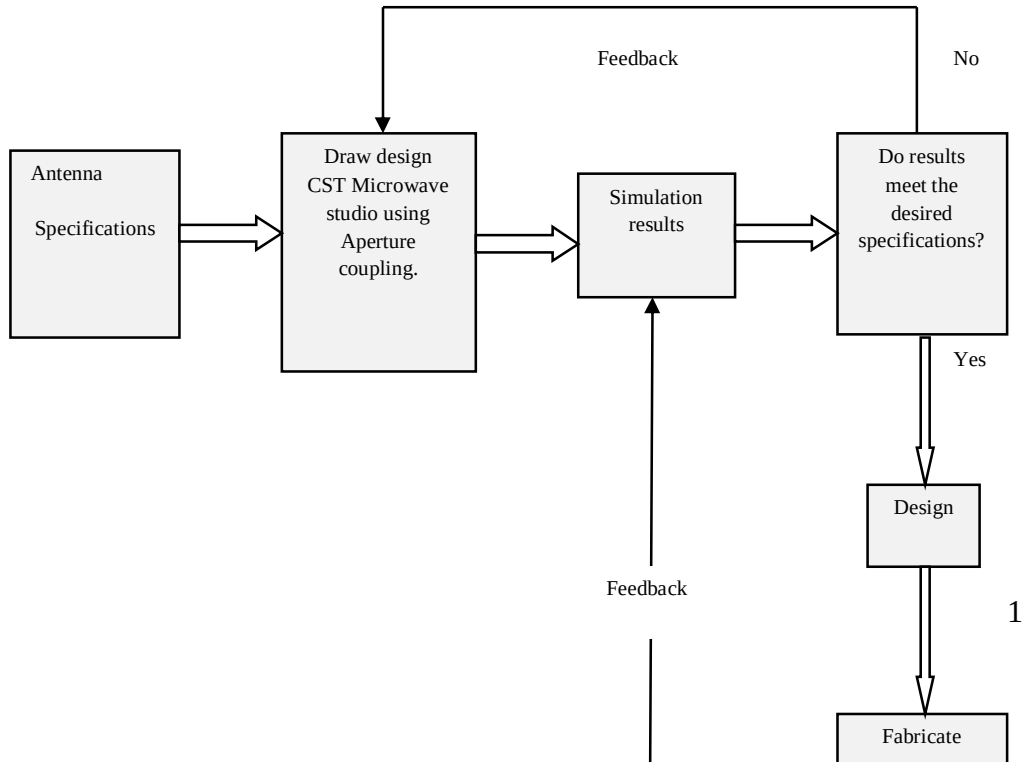

.

Figure 1.13: Flowchart for the antenna design.

1.6 Utilization of the Electromagnetic Spectrum for Wireless Communication Applications

For reference purposes, we include table 1.3 which gives an overview of the electromagnetic spectrum and its utilization for various wireless communication applications.

Table 1.3(Approximate Band Designations)

Approximate Band Designations	
L-band	1-2GHz
S-band	2-4GHz
C-band	4-8GHz
X-band	8-12GHz
Ku-band	12-18GHz
K-band	18-26GHz
Ka-band	26-40GHz
U-band	40-60GHz

Defense and space markets which emphasize on maximum performance gave an impetus to the development microstrip antennas and arrays in 1980s. However, applications of microstrip antennas in commercial sector are galloping most rapidly in 21st century. The microstrip antennas for commercial systems require low-cost materials, and simple and inexpensive fabrication techniques. Some of the commercial systems that presently use microstrip antennas are listed in the table1.4 [22] below

Table 1.4 (Application and allocated frequency)

Application	Frequency
Global positioning Satellite	1575MHz and 1227MHz
Paging	931-932 MHz
Cellular Phone	824-849 MHz and 869-895 MHz
Personal Communication System	1.85-1.99 GHz and 2.18-2.20 GHz
GSM	890-915 MHz and 935-960 MHz
Wireless Local Area Networks	2.40-2.48 GHz and 5.4 GHz
Cellular Video	28 GHz
Direct Broadcast Satellite	11.7-12.5GHz
Automatic Toll Collection	905 MHz and 5-6 GHz
Collision Avoidance Radar	60 GHz, 77 GHz, and 90 GHz
Wide Area Computer Networks	2.40-2.48 GHz and 5.4 GHz

1.7 Objective of the thesis

The objectives of the thesis are

- To study the basic principles of the Aperture coupled single band microstrip rectangular patch antenna.
- Design and simulation of wideband aperture coupled MPA.
- Parametric study of the proposed antenna.
- Design and simulation of dual band aperture coupled MPA.
- Parametric study of the proposed antenna.
- Fabrication of the designed antennas.

1.8 Thesis organization

The thesis is divided into five chapters.

Chapter 1 is dedicated to the Overview of Microstrip antenna.

Chapter 2 includes the literature survey on the aperture coupled antenna. The brief idea about the researches done for bandwidth enhancement, dual frequency, modeling of the aperture coupled antenna is given.

In Chapter 3, a single band antenna is designed and the effect of various physical parameters on the resonating frequency is studied.

In Chapter 4, the single band antenna is loaded with slots such that a dual frequency antenna is obtained.

Chapter 5 is dedicated to the conclusion and the future work.

Chapter 2

Literature survey on Aperture Coupled Microstrip Antennas

This chapter is devoted to the evolution of the aperture coupled antenna and its development in the recent past.

2.1 History of the Aperture Coupled Microstrip Antennas

The first aperture coupled microstrip antenna was fabricated and tested by a graduate student, Allen Buck, on August 1, 1984, in the University of Massachusetts Antenna Lab. This antenna used Duroid substrates with a circular coupling aperture, and operated at 2 GHz [19]. It was found that this antenna worked perfectly – it was impedance matched, and the radiation patterns were good. Most importantly, the required coupling aperture was small enough so that the back radiation from the coupling aperture was much smaller than the forward radiation level [22].

2.2 Progress of the Aperture Coupled Microstrip Antenna

Here we discuss in detail with references, some of the significant developments in the field of aperture coupled microstrip antennas.

2.2.1 Bandwidth enhancement in Aperture coupled microstrip antennas

One of the useful features of the aperture coupled microstrip antenna is that it can provide substantially improved impedance bandwidths due to the additional degrees of freedom offered by the stub length and coupling aperture size. While single layer probe or microstrip line-fed elements are typically limited to bandwidths of 2%-5%, aperture coupled elements have been demonstrated with bandwidths up to 10 - 15% with a single layer [25]-[27], and up to 30-50% with a stacked patch configuration [28]-[31]. Bandwidth can be enhanced by using H-shaped [32], L-shaped aperture in ground and by placing stubs in the patch [33], U-shaped slots in the patch [34]. A new technique to increase the bandwidth of slot antenna without increasing the volume of the antenna is obtained by using Z-slot and splitting the two side of the Z- slot into two or three fingers is proposed by C.-J. Wang and S.-W. Chang [35].

2.2.2 Dual frequency aperture coupled microstrip antennas

An overview about the dual-frequency techniques for patch antennas, Orthogonal-mode dual-frequency patch antennas, Multi-patch dual-frequency antennas, Reactively-loaded patch antennas, geometries for single and dual linear polarization, slotted rectangular-patch antenna, slotted cross-patch antenna, Cross-subarray dual-frequency patch antenna is discussed by S. Maci and G. BifJi Gentili [36]. A compact stack antenna consisting of square loop resonators, aperture couples, feed line and the perturbation for dual- band and circular polarization (CP) applications is proposed by J. C. Liu and B. H. Zeng, C. Y. Liu, H. C. Wu and C. C. Chang. This perturbation applies both dual-mode and orthogonal mode effects existing in the square loop resonator to present wide-band and circular polarization (CP) characteristics simultaneously [37].

An annular ring has also been used for dual frequency where the frequency for the propagating modes can be adjusted by choosing the inner and the outer radii. However, the ratio of the two frequencies is somewhat limited [38]. It is also possible to achieve dual frequency operation of a patch antenna by loading slots at both the resonating side and at the non-resonating side of the patch and by using shorting pins [39]-[40].

2.2.3 Antennas for WLAN and other wireless applications

A single fed aperture coupled antenna for WLAN application is designed and discussed by Rashid A. Saeed, S. Khatun, Borhanuddin, M. A. Khazani, Rania A. Mokhtar and Mahmoud Alshamary [41]. A dual-band antenna covering both the bands (2.45 and 5.2 GHz) for WLAN application is designed by combining a rectangular and two "*L*" shaped radiating elements embedding them on a single layer structure and achieved bandwidth of 30%and 20% while maintaining the structural compact size [42]. Multifrequency antenna for various wireless applications is designed by using manifold slot structures like the printed slot, the slotted form and inverted-L slot[43], fractal shapes [44][45][46], polygon patch [47].

2.2.4 Modeling of aperture coupled microstrip antennas

Analysis of the aperture coupled microstrip element is complicated by the presence of two dielectric layers, and the microstrip line-to-slot transition. The initially the aperture coupled element [19] presented a simplified cavity-type model, Sullivan and

Schaubert [48] analyzed it using a full-wave moment method solution. D M Pozar used the reciprocity theorem to analyze the aperture coupled antenna [49]. Moment method analysis techniques are versatile and highly accurate but take relatively long simulation times. Cavity models, are more approximate requiring negligible computer resources. Some examples of cavity models for aperture coupled microstrip antennas include [50]-[51]. The numerical techniques like Green's Functions, Mixed Potential Integral Equations and Method of Moments used for the analysis of coupled antenna are discussed by D. Yau and N. V. Shuley [52].

The basic Finite-difference time-domain FDTD space grid and time-stepping algorithm trace back to a seminal 1966 paper by Kane Yee [14]. An improved Finite-difference time-domain (FDTD) based on novel integral transform and the matrix theory method has been extended to analyze the antennas with complicated lumped/active networks [53]. A polarimetric scattering from two-dimensional (2-D) rough surface is presented by the Finite-difference time-domain (FDTD) algorithm [54]. Also, a new FDTD time-to-frequency domain conversion algorithm based on the optimization of non-uniform fast Fourier transform (NUFFT) is presented by Y.-H. Liu and Q. H. Liu and Z.-P. Nie [55].

2.2.5 Antenna with defected ground structure (DGS)

Multibanding of the antenna is also possible by using defected ground structure (DGS) which disturbs the shield current distribution in the ground plane which further influences the input impedance and current flow of the antenna providing a bandpass or bandstop like filter and other microwave circuits [56] [57]. Method of calculating the characteristics impedance of transmission line with DGS is given by J. Lim, J. Lee, J. Lee, S.-M. Han, and D. Ahn. and Y. Jeong [58].

Thus, in many applications, operation at two or more discrete bands with an arbitrary separation of bands is desired. In such cases, a patch capable of operating in multiple bands is desirable. For most applications, all bands may be required to have the same polarization, radiation pattern, and bandwidth characteristics. Multi-banding of an antenna can be done by using fractal shapes [44][45][46], polygon patch [47], E-shape, V-shape and U-shape patches [2],[6],[60]. One method is to use separate patches abreast each other for different applications. Arraying of the antenna can also be done but it increases the size of the antenna. Stacking of the patches can also be used but it increases the volume of the antenna. It is also desirable to have one port

and an arbitrary separation of the frequency bands. All of these requirements impose severe constraints on the use of natural modes [39]. An annular ring has also been used for dual frequency where the frequency for the propagating modes can be adjusted by choosing the inner and the outer radii. However, the ratio of the two frequencies is somewhat limited [38]. It is also possible to achieve dual frequency operation of a patch antenna by loading slots at both the resonating side and at the non-resonating side of the patch and by using shorting pins [39]-[40].

In the proposed design, two slots are loaded at the patch to make it to dual frequency antenna without increasing the volume unlike stacking of patches. Also, the fabrication process of the slot is compatible with antenna fabrication technology.

Chapter 3

Single band Aperture Coupled antenna Design and its parametric study

This chapter covers the basics of aperture coupling and the transmission line model parameters of the proposed antenna are calculated. Firstly a single band antenna is designed for WLAN applications at a frequency of 2.40GHz. The effect of various parameters like patch width, patch length, dimensions and position of aperture etc… on the designed antenna is described. An antenna with dumbbell shaped aperture in the ground is also designed.

3.1 Basics of Aperture coupled antenna

In 1985, a new feed technique involving a microstrip line electromagnetically coupled to a patch conductor through an electrically small ground plane aperture was proposed. The figure 3.1 shows the pictorial view of the aperture coupled antenna

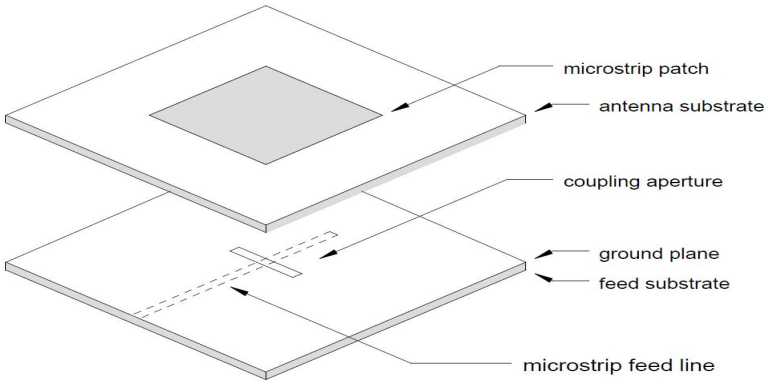

Figure 3.1: Pictorial view of the aperture feed

As stated in chapter 1 that an aperture coupled antenna eliminates direct electrical connections between the feed conductor and radiating patch, and the ground plane electrically isolates the two structures. The two dielectric substrates can be selected independently to optimize both microstrip guided waves and patch radiating waves. Generally, the antenna substrate is thicker and has a lower dielectric constant than the feed substrate. Aperture coupled antennas are advantageous in arrays because they electrically isolate the feed and phase shifting circuitry from the patch antennas. The disadvantage is the required multilayer structure which increases fabrication complexity and cost. Figure 3.2 shows the aperture coupled microstrip antenna in

block diagram form. The feed line creates an electric field in the aperture (ground plane slot), which induces surface currents on the patch. The patch edges perpendicular to the feed line create fringing fields that radiate into free space.

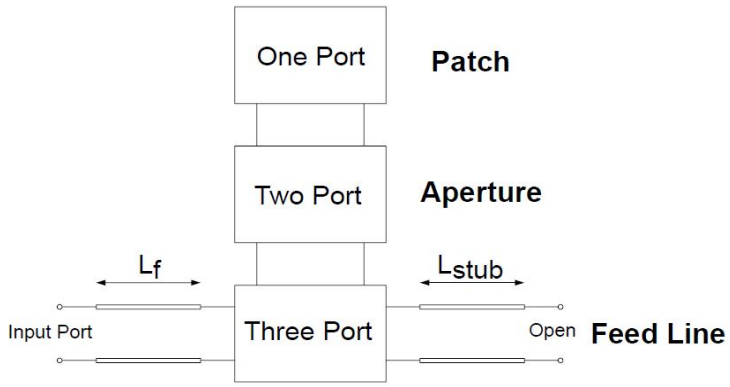

Figure 3.2 Aperture coupled antenna block diagram [61]

3.2 Equivalent circuit of Aperture Coupled antenna

The equivalent circuit of the aperture coupled antenna is shown in the figure 3.3.The ground plane slot acts as an impedance transformer and parallel LC circuit (L_{ap} and C_{ap} in Figure 3.3) in series with the microstrip feed line [61]. The LC circuit represents the ground plane slot resonant behavior. The N:1 impedance transformer represents the patch antenna's impedance effects being coupled through the ground plane slot. The patch is modeled as two transmission lines terminated by parallel RC components (R_{rad} and C_{fring}) due to patch edge fringing fields.

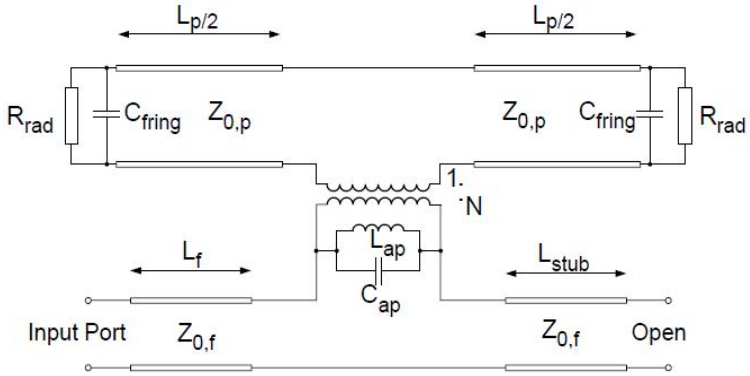

Figure 3.3 Transmission equivalent circuit of the antenna [61]

The antenna circuit model parameters are determined from equations (3.1) through (3.8)

$$\varepsilon_{eff} = \frac{\varepsilon_r + 1}{2} + \frac{\varepsilon_r - 1}{2}\left(1 + \frac{10\mathbf{H}}{\mathbf{W}}\right)^{-0.5} \quad (3.1)$$

$$\Delta = 0.412\mathbf{H}\left(\frac{\varepsilon_{eff} + 0.300}{\varepsilon_{eff} - 0.258}\right)\left(\frac{\frac{\mathbf{W}}{\mathbf{H}} + 0.262}{\frac{\mathbf{W}}{\mathbf{H}} + 0.813}\right) \quad (3.2)$$

$$G = \frac{\pi W}{\eta \lambda_o}\left(1 - \frac{\left(\frac{2\pi H}{\lambda_o}\right)^2}{24}\right) \quad (3.3)$$

$$B = 0.01668\frac{\Delta}{H}\left(\frac{W}{\lambda_o}\right)\varepsilon_{eff} \quad (3.4)$$

$$R_{rad} = \frac{1}{G} \quad (3.5)$$

$$C_{fringe} = \frac{B}{2\pi f} \quad (3.6)$$

$$Z_o = \frac{\frac{120\pi}{\sqrt{\varepsilon_{eff}}}}{\frac{\mathbf{W}}{\mathbf{H}} + 1.393 + 0.667\ln\left(\frac{\mathbf{W}}{\mathbf{H}} + 1.444\right)} \quad (3.7)$$

$$L_{ap}C_{ap} \sim \left(\frac{1}{2\pi f}\right)^2 \quad (3.8)$$

The antenna circuit model parameters for the antenna designed in section 3.3 are tabulated in the table 3.1

Table 3.1(Antenna transmission line model parameters)

S.No.	Variable	Value
1	f_r (Operating frequency)	2.43GHz
2	λ_r (Free space wavelength)	0.1234 m
3	η_o (Free space impedance)	377ohm
4	ε_r (Substrate dielectric constant)	2.20
5	$\varepsilon_{p,eff,}$ (Patch effective relative dielectric constant)	2.08

6	$\varepsilon_{f,eff,}$ (Feed effective relative dielectric constant)	2.46
7	W_p (Width of Patch)	46 mm
8	H_p (Height of Patch substrate)	2.402 mm
9	W_f (Width of feed)	6 mm
10	H_p (Height of Patch substrate)	2.402 mm
11	Δ (Field extension due to fringing)	1.2 mm
12	G (Parallel plate radiator conductance)	0.0030 S
13	B (Fringing field capacitive susceptance)	0.0064 S
14	$Z_{o,p}$ (Line impedance of patch)	11.59
15	$Z_{o,f}$ (Line impedance of feed)	50.07
16	R_{rad} (Fringing field resistance)	323.62 ohm
17	C_{ap} (Aperture capacitance)	22.45 pF
18	L_{ap} (Aperture inductance)	191.1 pF
19	C_{fringe} (Fringing field capacitance)	0.419 pF
20	N (Impedance transformer turns ratio)	1.53

3.3 Single band antenna design

Firstly, a single band antenna consisting of a rectangular patch, rectangular aperture and feed line was designed for WLAN application. The dimensions of the antenna were calculated as per the equations given in CA Balanis [6].

Table 3.2(Dimensions of the unoptmized antenna)

S. No	Parameters	Value
1	f_r (Resonating frequency)	2.42GHz
2	L_p (Length of patch)	40 mm
3	W_p (Width of patch)	48 mm
4	L_g (Length of Ground)	40 mm
5	W_g (Width of ground)	48 mm
6	H_a(Height of Antenna Substrate)	2.4 mm
7	H_f (Height of Substrate)	2.4 mm
8	W_f (Width of feed)	7.39 mm

9	L_f (Length of feed)	22.65 mm

The aperture dimensions are taken such that the ratio of width to length of the aperture is 1/10.

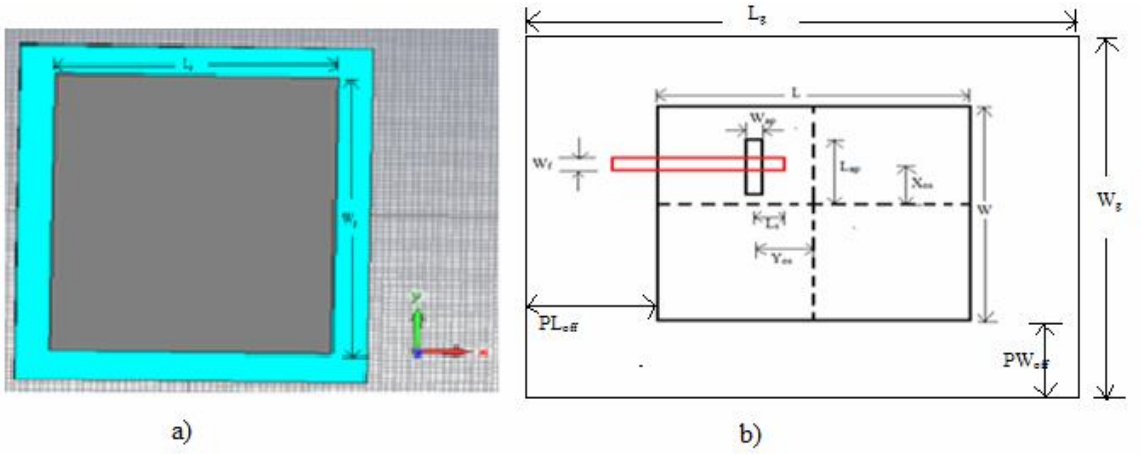

Figure 3.4: a) Front view of antenna b) Dimensional diagram of antenna.

The figure 3.4 shows us the front view of the unoptmized antenna which is excited by a Gaussian pulse at the waveguide port as shown in figure 3.5.

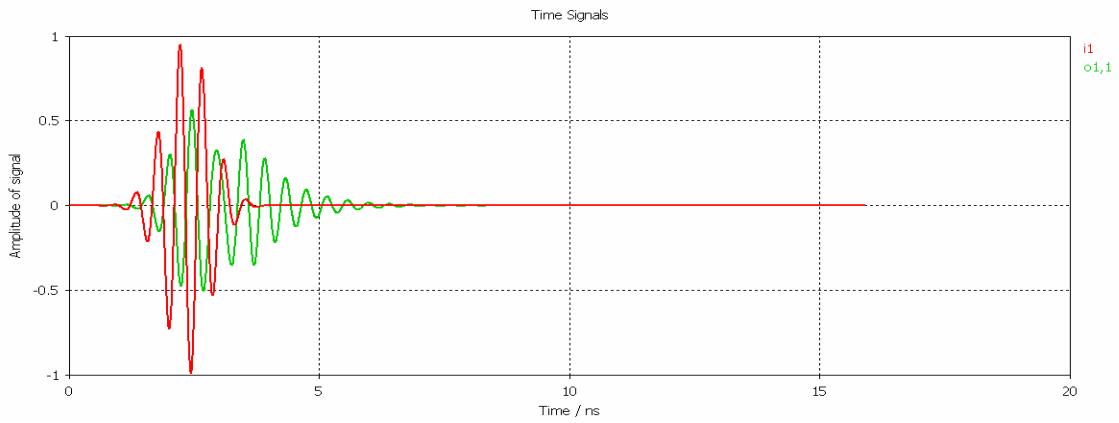

Figure 3.5: The Simulations time signals

The figure 3.6 shows the S-parameters as a function of frequency

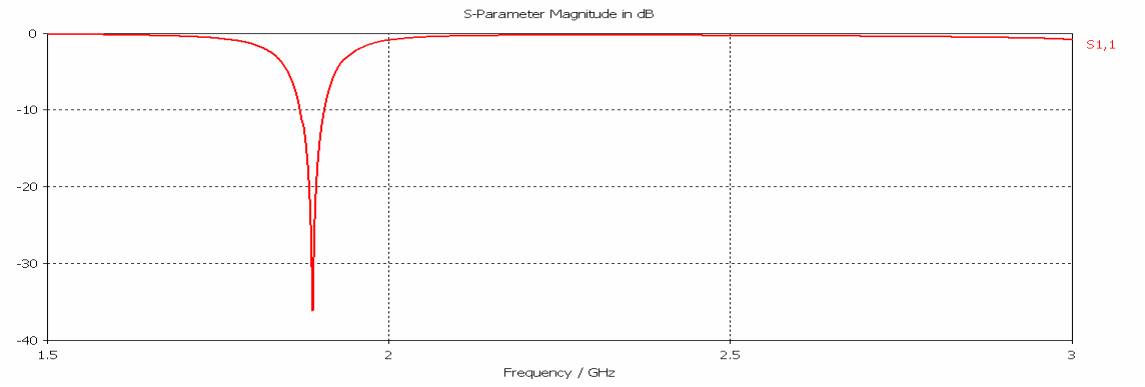

Figure 3.6: S-parameter of the test antenna

From the figure 3.6, it is observed that the antenna resonates at 1.76 GHz which is not the desired frequency. Hence, we have to vary our parameters so that an optimized antenna with desired bandwidth and frequency can be designed.

3.4 Physical Parametric Study of the antenna

In this section, the effect of the various physical parameters like patch length, patch width, aperture dimensions, antenna and feed substrates, feed line dimensions etc…are studied, by varying one parameter at a time and keeping all other parameters constant so that one can get an optimized antenna for the desired applications.

3.4.1 Effect of Patch length

The patch length affects the resonating frequency of the antenna.

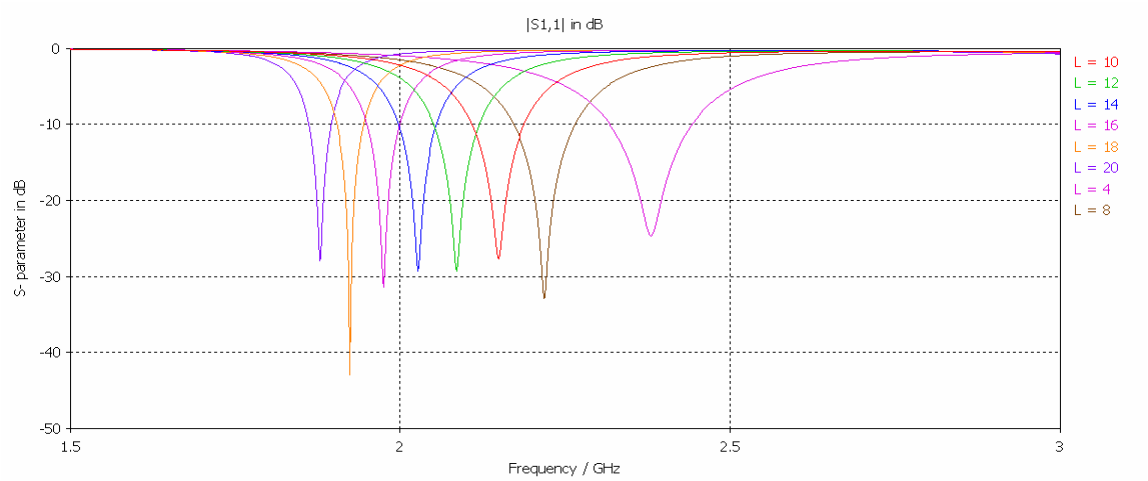

Figure 3.7: Variation of S-parameter w.r.t patch length

As the patch length is changed from 40 mm to 24mm, it is observed from the figure 3.7 and table 3.3 that the resonating frequency changes from 1.87 GHz to 2.38 GHz. So, a patch length of 25 mm is chosen. Now, the position of the patch is varied such the antenna resonates at the 2.42 GHz.

Table 3.3 (Resonating frequency for various patch lengths)

Length of patch (in mm)	40	38	36	34	32	30	28	24
Resonating freq. (in GHz)	1.87	1.92	1.97	2.02	2.08	2.14	2.22	2.38

3.4.2 Effect of patch position along resonating (x-axis) direction

Moving the patch relative to the aperture in the E-plane decreases the coupling level. It can be seen from the figure 3.8 that, when the value of patch length offset (PL_{off}= 25 + LoP) is increased from 15 mm to 14 mm the magnitude of S11 parameter approaches from -20.95 dB to -38.97 dB.

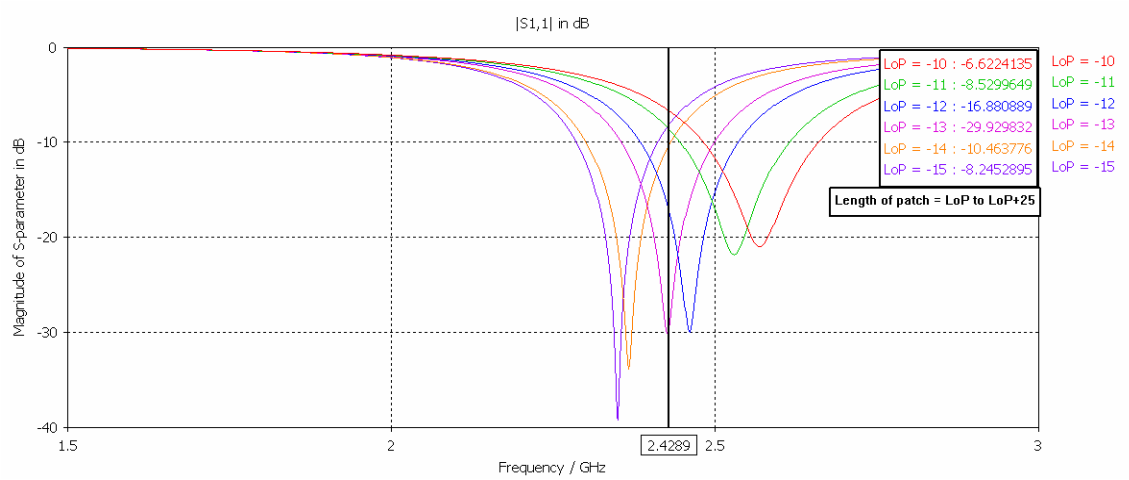

Figure 3.8: Variation of S-parameter w.r.t patch position along resonating direction.

From the figure 3.8 and table 3.4, the patch position is selected such that the maximum coupling takes place at the desired frequency. Table 3.4 shows the variation of coupling level and resonating frequency with change in the patch length offset.

Table 3.4 (Variation of S11 with position of patch)

Patch length offset (PL_{off}) in mm	15	14	13	12	11	10
S11(in dB)	-20.95	-21.62	-29.55	-29.92	-33.49	-38.97
Resonating freq. (in GHz)	2.56	2.53	2.46	2.42	2.36	2.34

The position of the patch with PL_{off} equals to 12 mm is depicted in the figure 3.9.

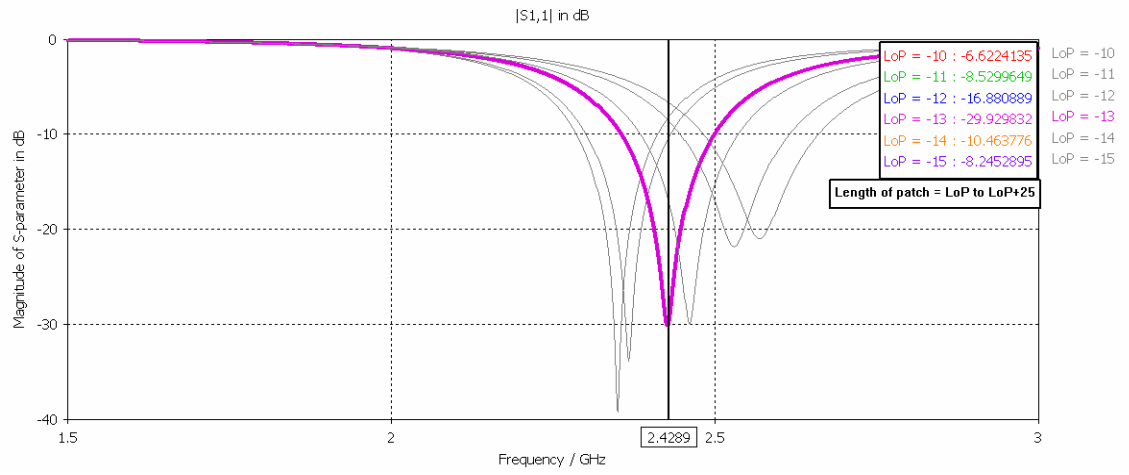

Figure 3.9: Selected patch position for maximum coupling.

3.4. 3 Effect of patch width

The width of the patch affects the resonant resistance of the antenna, with a wider patch giving a lower resistance. Square patches may result in the generation of high cross polarization levels, and thus should be avoided unless dual or circular polarization is required. The variation in the input impedance of the antenna is shown in the figure 3.10

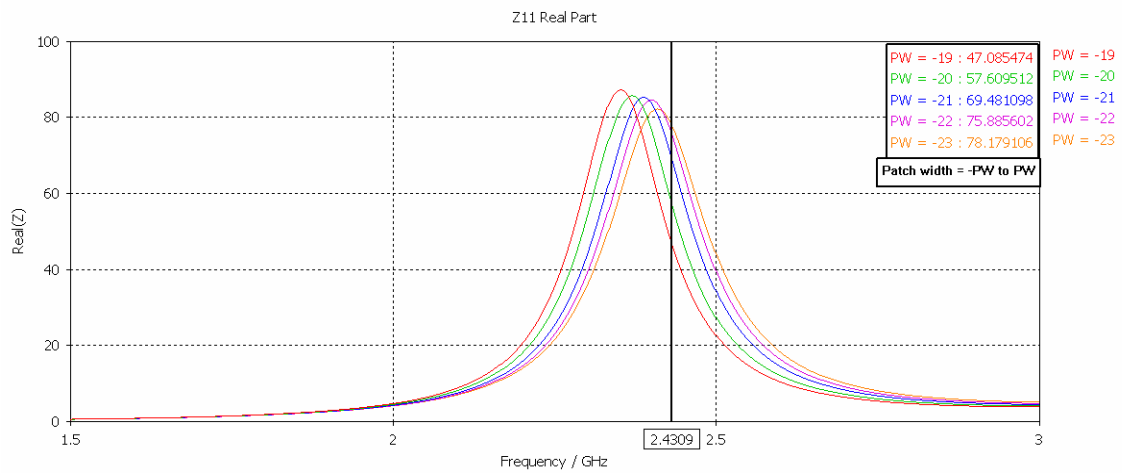

Figure 3.10: Variation of real (Z) w.r.t patch width.

It is observed from the figure 3.10 and table 3.5 that as the patch width increases from 38 mm to 46 mm the input impedance decreases 85 to 75.88 ohm.

Table 3.5(Variation of input impedance with change in the patch width)

Patch width (in mm)	38	40	42	44	46
Real (Z11)(in ohm)	85	84	82	83	79
Resonating freq.(in GHz)	2.36	2.38	2.40	2.41	2.295

The patch width of 46 mm is selected having the input impedance of 78.17 ohm is shown in the figure 3.11:

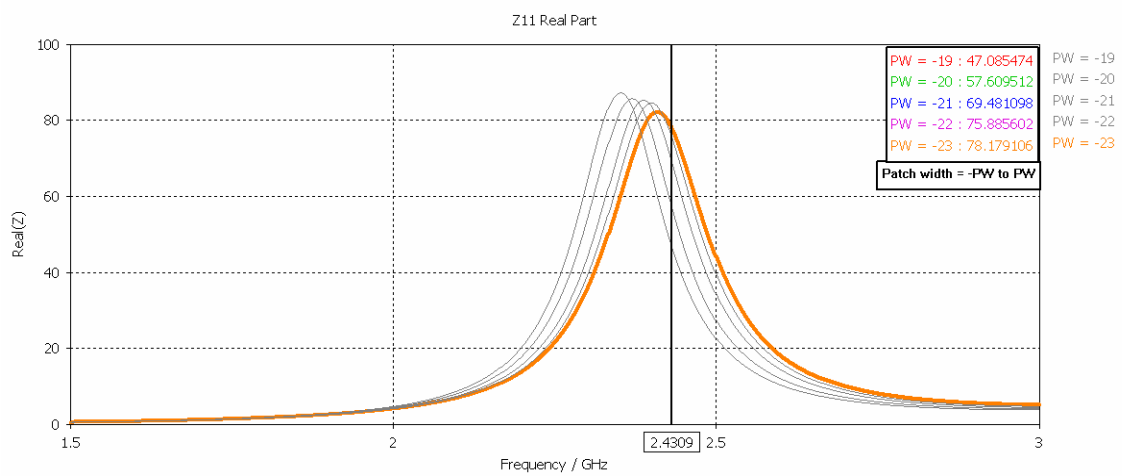

Figure 3.11: Selected patch width with its input impedance.

3.4.4 Effect of patch position along non-resonating (y-axis) direction

Moving the patch relative to the slot in the H-plane direction has little effect on the resonating frequency and the coupling level. The figure 3.12 depicts the change in the S-parameter when patch is varied along the y-axis keeping the patch width fixed to 46 mm.

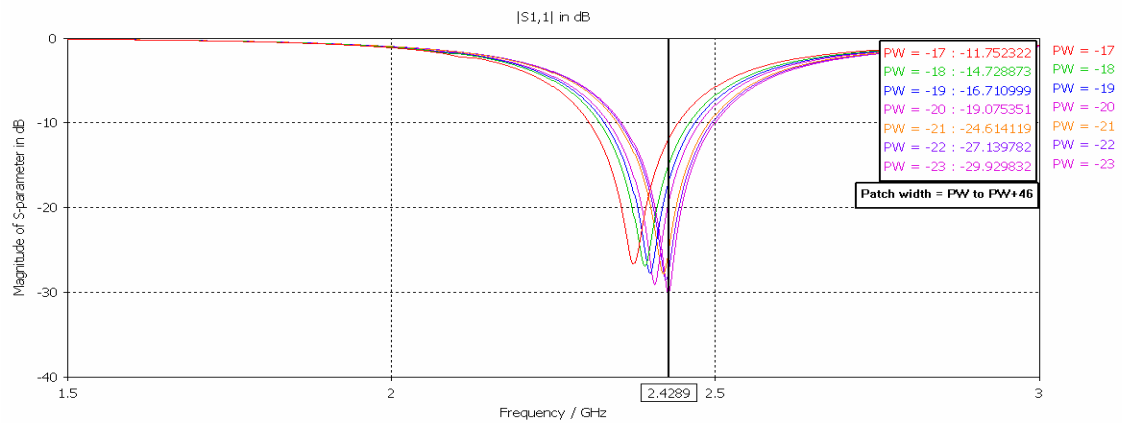

Figure 3.12: Variation of S-parameter w.r.t patch position along non-resonating direction.

3.4.5 Effect of Aperture length

The coupling level is primarily determined by the length of the coupling aperture, as well as the back radiation level. The aperture should therefore be made no larger than is required for impedance matching.

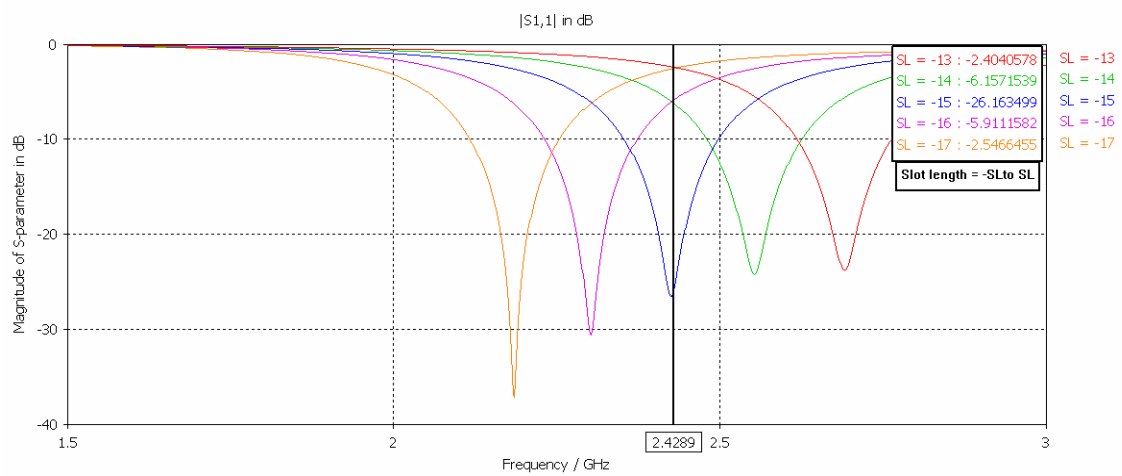

Figure 3.13: Variation of S-parameter with change in Slot length

When the aperture length (slot length) is increased from 26 mm to 34 mm keeping the slot width to slot length ratio to 1/10, there is a decrease in the coupling level. So, the slot length equal to 30 mm is selected as depicted in figure 3.13.The slot length also affects the input impedance of the antenna. The variation in the real part of Z11 is shown in the figure 3.14:

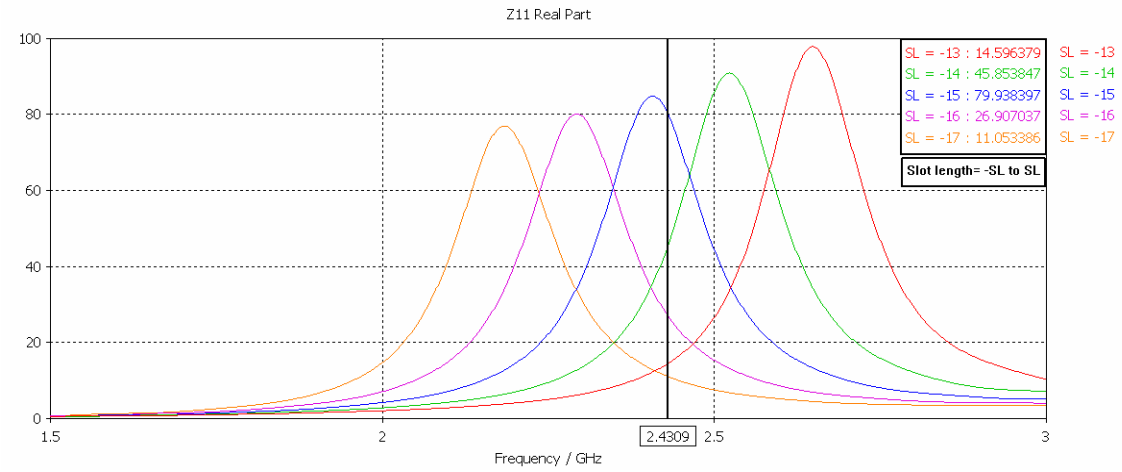

Figure 3.14: Variation of real (Z11) with change in slot length.

From figure 3.14 and table 3.6, it is revealed that the real part of Z11 decreases as the slot length increases from 26 mm to 34 mm. So, the slot length chosen for the good impedance is 30 mm covering the desired frequency band. The table 3.6 shows the variation in the resonating frequency, magnitude of S-parameter and real Z11with change in the aperture length.

Table 3.6 (Variation in the resonating frequency, magnitude of S-parameter and real Z11with change in the aperture length)

Patch width (in mm)	26	28	30	32	34
Mag. of S11(in dB)	-23.75	-23.52	-26.50	-30.56	-36.30
Resonating freq.(in GHz)	2.69	2.55	2.43	2.30	2.18
Real of Z11(ohm)	97	89	84	80	76

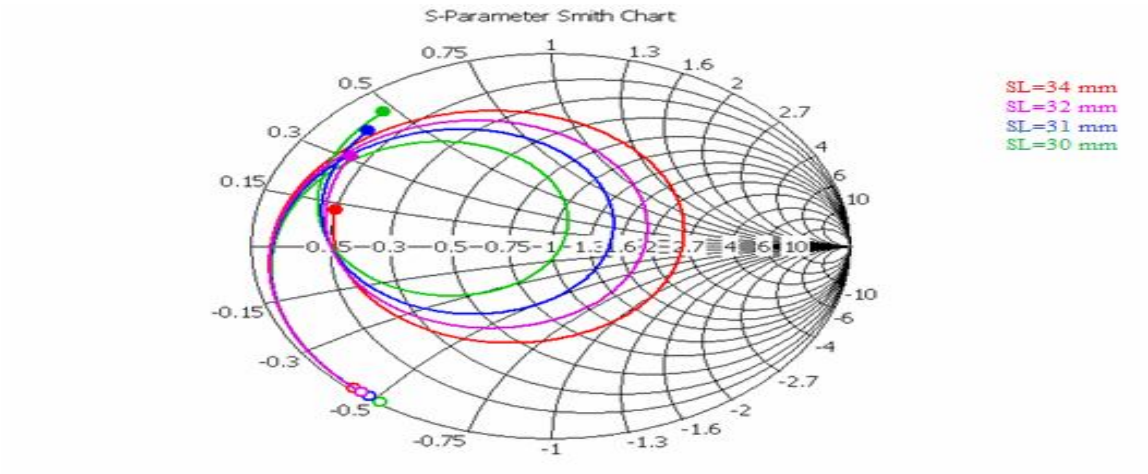

Figure 3.15: Smith chart variation with change in aperture length

From figure 3.15, it is concluded that the size of the locus of the smith chart is controlled by the slot length. As the slot length increases, the size of the locus increases. For proper matching the locus must be large enough that it passes through the centre of the smith chart. Hence, slot length has to be chosen properly. Here, for the desired frequency band the slot length chosen is 30mm. Now once the slot length equal to 30mm is selected, figure 3.16 shows the effect of position of the slot length.

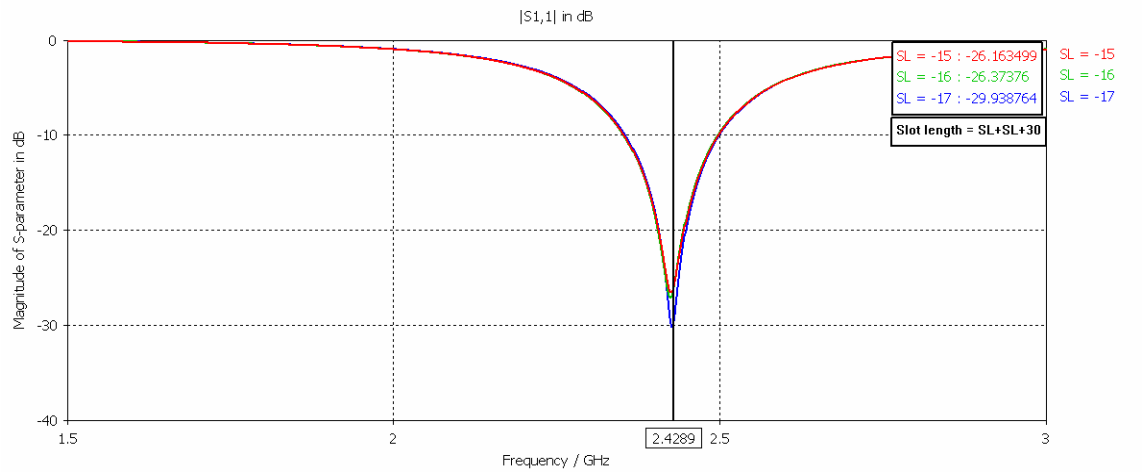

Figure 3.16: Effect of position of aperture on S-parameter.

When the aperture is moved along the non-resonating side, there is hardly any effect on the S-parameter. From the figure 3.16, the position of the aperture is selected along non-resonating side.

3.4.6 Effect of Aperture (slot) width

When the aperture width (width of slot) is increased from 1 mm to 4 mm keeping the aperture length and position fixed as in section 3.4.5, the coupling level of the antenna is decreased. So the aperture width equal to 3 mm is chosen such that slot width to slot length ratio is 1/10.

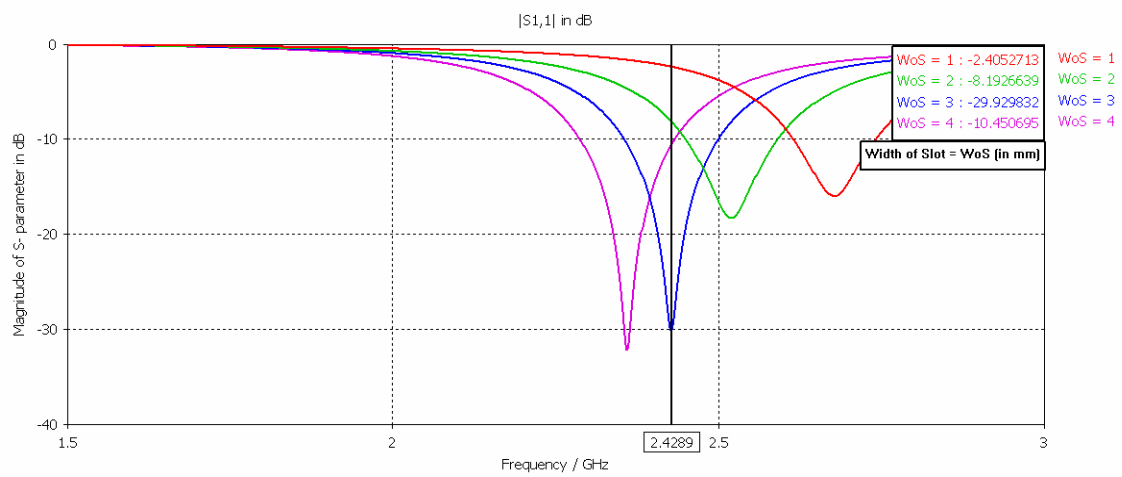

Figure 3.17: Variation of S-parameter with change in width of slot.

Figure 3.17 and table 3.7 shows the variation of the S-parameter with change in the width of slot.

Table 3.7(Variation of the S-parameter with change in the width of slot)

Width of slot (in mm)	1	2	3	4
Mag. of S11(in dB)	-15.87	-18.20	-30.08	-32.10
Resonating freq. (in GHz)	2.683	2.52	2.427	2.35

Figure 3.18 shows the affect of the change in the position of aperture along the resonating side of the antenna when the slot width is fixed to 3 mm.

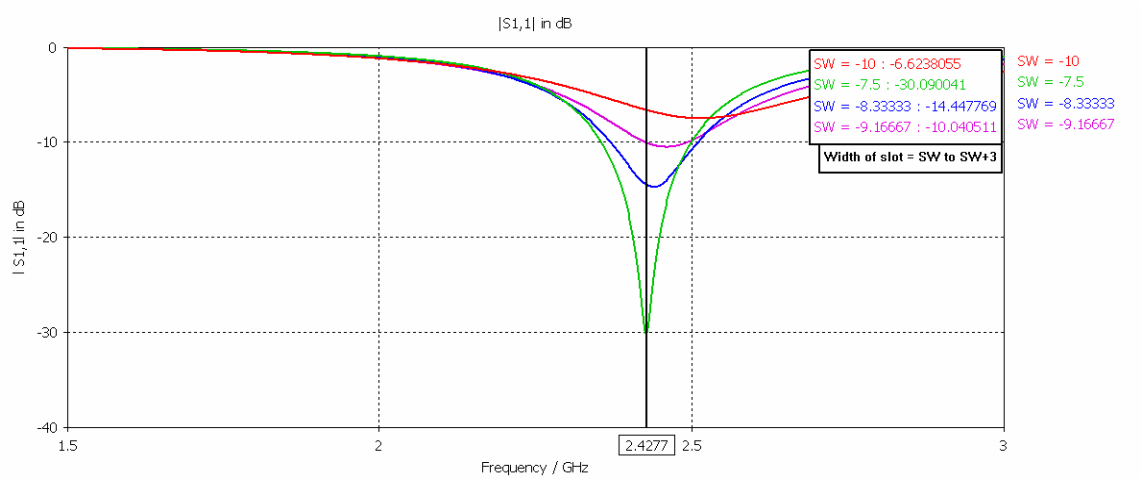

Figure 3.18: Variation of S-parameter with change in aperture position along resonating side.

From the figure 3.18, the position of the aperture along the resonating side of the patch is selected such that maximum coupling takes place.

3.4.7 Effect of feed line length or length of stub

The length of feed line also affects the coupling level. When the feed line length is increased from 22 mm to 26.5 mm as shown in figure 3.19, there is a decrease in the coupling level from -8.42 dB to -30.08 dB at 2.4287 GHz. So, for proper matching length of the feed line chosen is 23.5 mm which corresponds to a stub length of 4.5 mm.

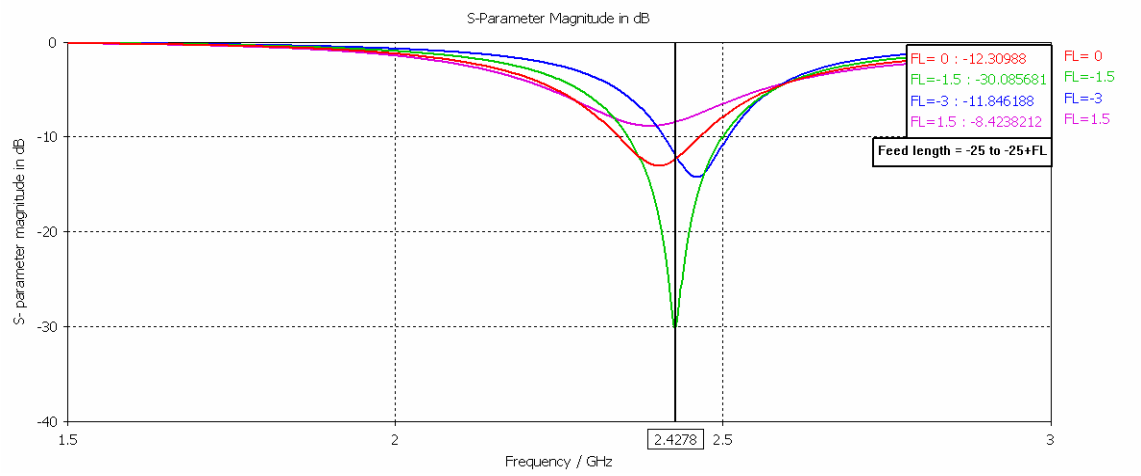

Figure 3.19: Variation of S-parameter with change in length of feed line.

Also, the stub length is used to rotate the entire locus up (inductive) or down (capacitive) on the Smith chart. When the feed line length is increased from 22 mm to 25 mm (i.e. the stub length is increased from 3 mm to 7.5 mm), the locus of the Smith

chart is rotating towards inductive side. Figure 3.20 shows the effect of increasing the length of the stub.

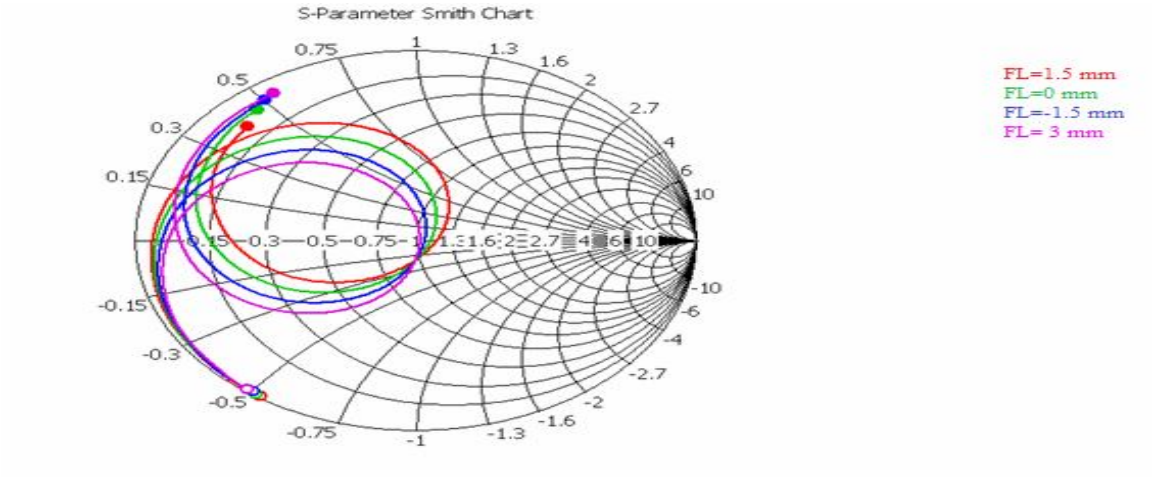

Figure 3.20: Smith chart variations with change in feed line length.

Thus, for optimum matching, where the locus is just large enough to pass through the center of the Smith chart can be obtained by properly adjusting the slot length and the stub length.

3.4.8 .Effect of feed line width

The width of the feed line controls the line impedance of the feed. Figure 3.21 shows that with increase in the width from 2 mm to 6 mm, the line impedance changes from 145.7 ohm to 74.86 ohm.

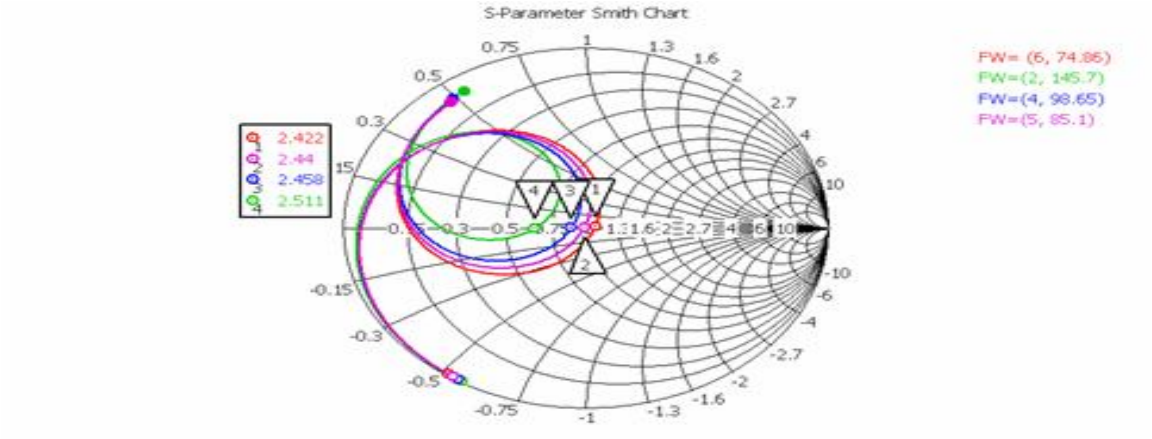

Figure 3.21: Smith chart variations with change in feed line width.

Also, the coupling level is affected by varying the feed line width. Figure 3.22 shows that with increase in the width of feed line from 2 mm to 6 mm, the coupling increases.

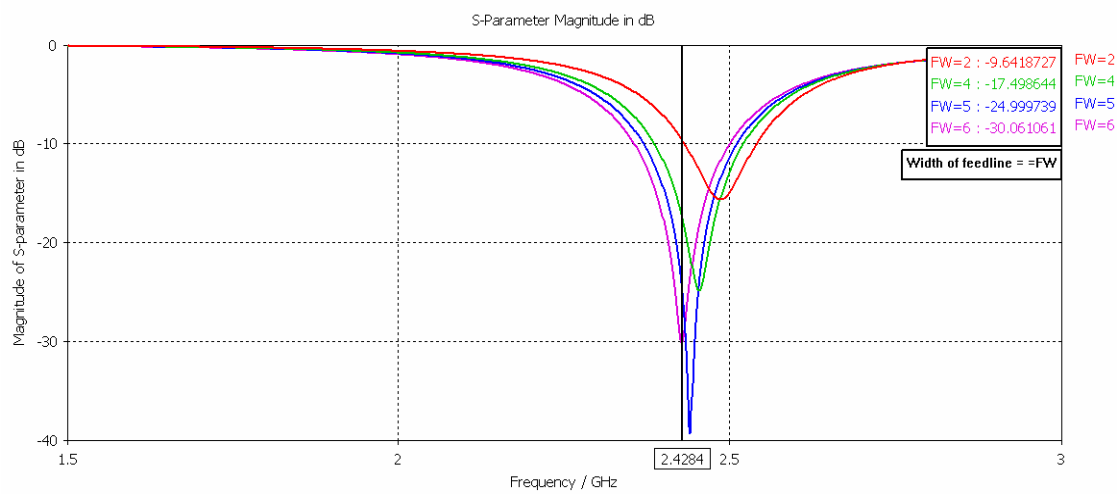

Figure 3.22: Variation of S-parameter with change in width of feed line.

Thus, for the desired frequency band the width of feed line selected is 6 mm.

3.4.9 Effect of height of antenna substrate

Now the height of antenna substrate is increased from 1.6 mm to 3.2 mm keeping the other parameters same as selected in above sections. Figure 3.23 shows that with increase in the height of the antenna substrate the bandwidth of the antenna increases.

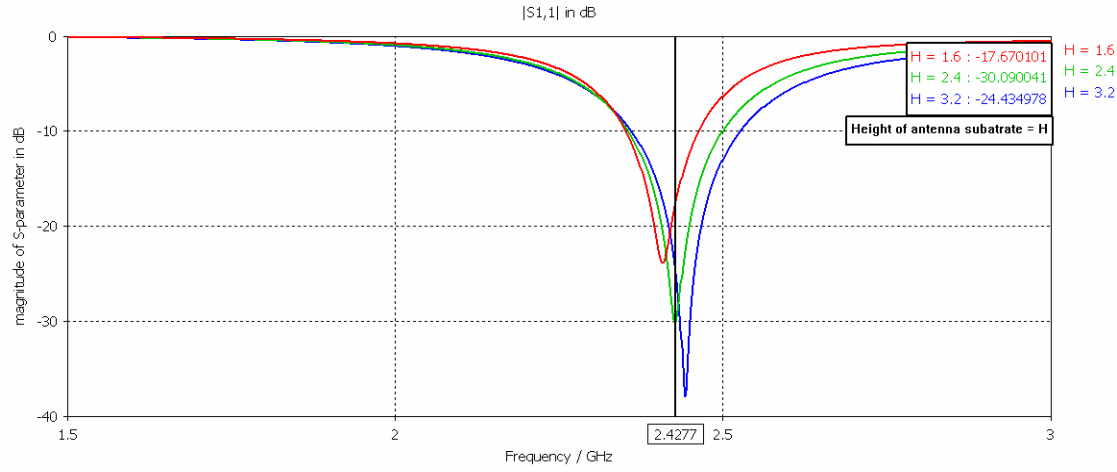

Figure 3.23: Variation of S-parameter with change in height of antenna substrate.

3.4.10 Effect of changing the Antenna and Feed substrates

The resonating frequency of the antenna is dependent on the dielectric constant of the substrates. The figure 3.24 shows that as the dielectric constant increases the resonating frequency of the antenna decreases.

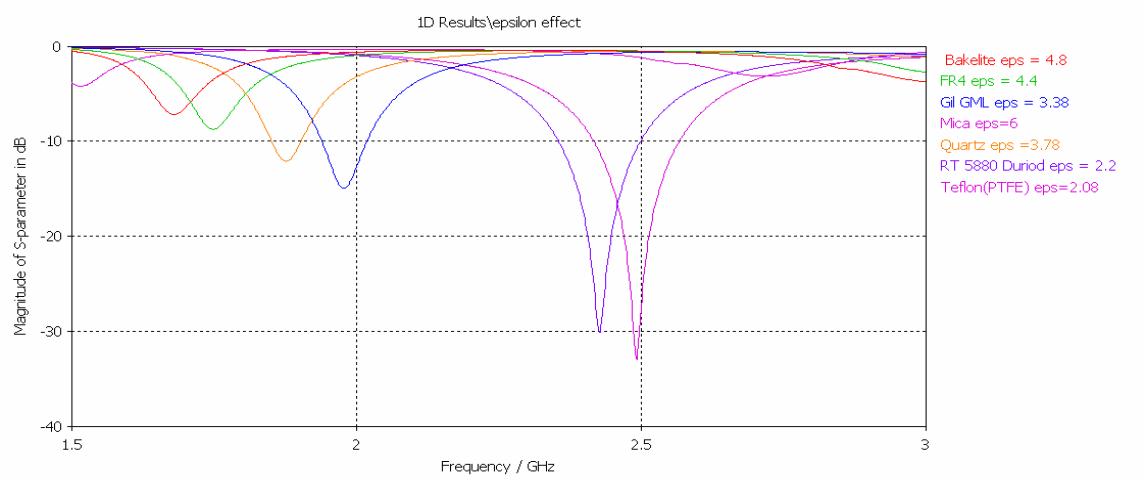

Figure 3.24: Variation of resonating frequency with change in the dielectric constant of both substrates.

The table 3.8 shows that as the dielectric constant of the two substrates increases there is a decrease in the resonating frequency.

Table 3.8(Dielectric constant v/s resonating frequency)

Dielectric constant	2.08	2.2	3.38	3.78	4.4	4.8	6
Resonating freq. (in GHz)	2.49	2.43	1.97	1.87	1.74	1.67	1.51

3.4.11 Effect of changing the feed substrate keeping duroid as antenna substrate

Generally, a high dielectric constant is used for the feed substrate so that the radiations can be optimized. Hence, in this section the feed substrate is assigned various materials like FR4, PTFE, Quartz etc keeping the antenna substrate as duroid and the change in the resonating frequency are shown in the figure 3.25.

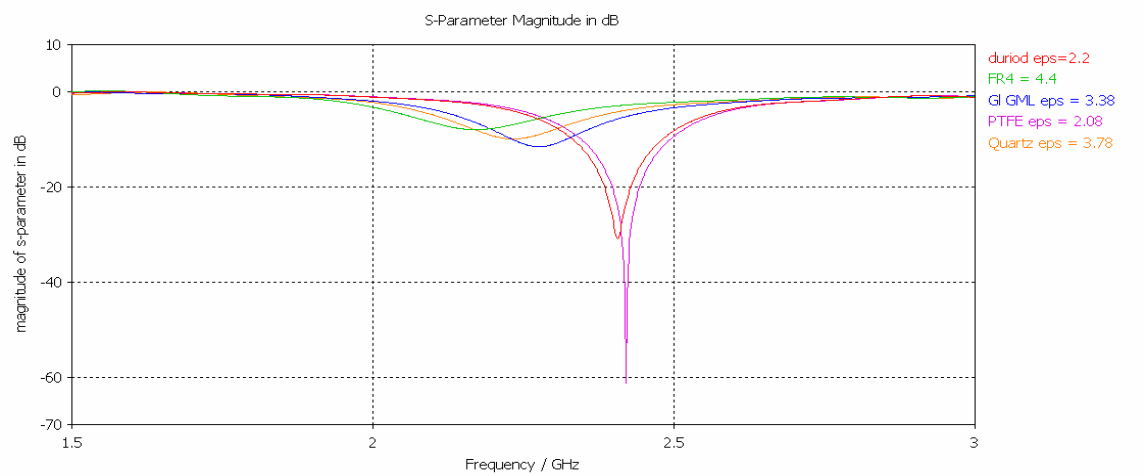

Figure 3.25: Variation in resonating frequency with change in the feed substrate.

As the feed line is etched on the feed substrate, the line impedance of the feed is also changed. Table 3.9 shows the change in the resonating frequency and the line impedance of the antenna with change in the feed substrate.

Table 3.9(Dielectric constant of feed substrate v/s Line impedance)

Dielectric constant of feed substrate	2.08	2.2	3.38	3.78	4.4
Resonating frequency(in GHz)	2.41	2.406	2.27	2.229	2.14
Line impedance(in ohm)	76.7	74.7	60.13	57.71	53.2

Figure 3.26 shows that as the dielectric constant of the feed substrate is increased from 2.2 (duroid) to 4.4 (FR4), the line impedance decreases from 74.86 ohm to 53.2 ohm and the locus size increases making the impedance inductive.

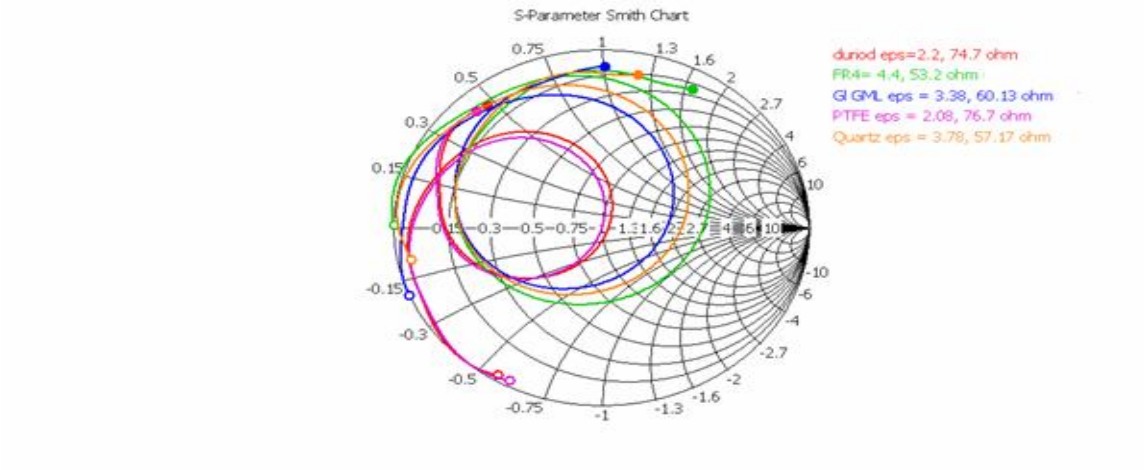

Figure 3.26: Smith chart variations with change in feed substrate.

3.4.12 Effect of aperture shape (Defected ground structure)

Usually, a designer of microstrip circuits focuses on the analysis, synthesis, and calculation of the microstrip circuit (conductor trace), including configuration, dimensions, and structure of the microstrip conductor, while the ground side remains a complete metallization structure. However, the ground plane structure can be modified to improve electrical performance and reduce size of a microstrip circuit. In recent years, there have been several new designs of microstrip circuits with defected ground structure (DGS) [55- 62]. Microstrip lines with DGS have much higher impedance and an increased slow-wave factor as compared to conventional transmission lines. The DGS is attractive as it enables unwanted frequency rejection and circuit size reduction. The DGS is a new type of microstrip design that exhibits well-defined stop bands and pass bands in the transmission characteristics, and as such it finds many applications in microwave printed circuits: filters, dividers, amplifiers, oscillators, switches, directional couplers, antennas, etc.

The DGS applied to a microstrip line creates a resonance in the circuit, with the resonant frequency controllable by changing the shape and the size of the slot .The equivalent circuit of the DGS can be represented by a parallel *LC* resonant circuit in series with the microstrip line. The transverse slot in the DGS increases the effective capacitance, while the U-shaped slots attached to the transverse slot increase the effective inductance of the microstrip line. This combination of DGS elements and microstrip lines yields sharp resonances at microwave frequencies which can be controlled by changing shape and size of the DGS circuitry. The shape and size of the DGS slot controls both the fundamental resonant frequency and higher order resonances. The size of the PCB area is also considered. To fulfill the different requirements, a variety of DGS shapes have evolved over time, including dumbbell, circular, bow-tie, hourglass and H-shaped structures. Figure 3.27 shows the commonly used rectangular and dumbbell shape of the aperture.

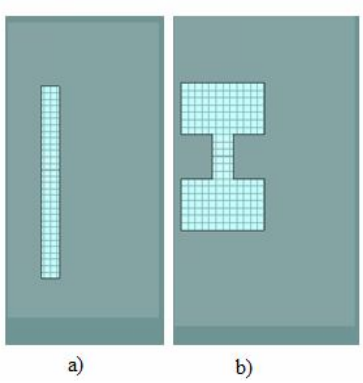

Figure 3.27: a) Rectangular aperture b) Dumbbell shape etched on the ground plane.

In the antenna designed in section 3.4, a dumbbell shape is etched keeping all other parameters fixed. The figure 3.28 shows the S-parameter of the antenna.

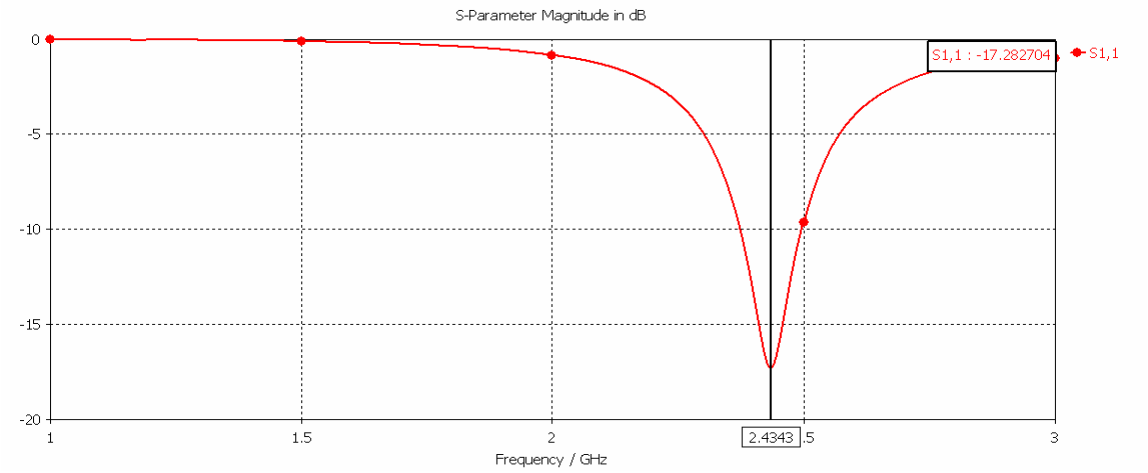

Figure 3.28: S-parameter of the antenna.

Figure 3.28 shows that the minimum value of S11 at 2.4343 GHz is -17.28 dB. It has a 10 dB down bandwidth of 120 MHz covering WLAN band 2.40 GHz-2.48 GHz. Figure 3.29 the VSWR of the antenna is shown. The VSWR of the antenna at 2.4343 GHz is 1.31.

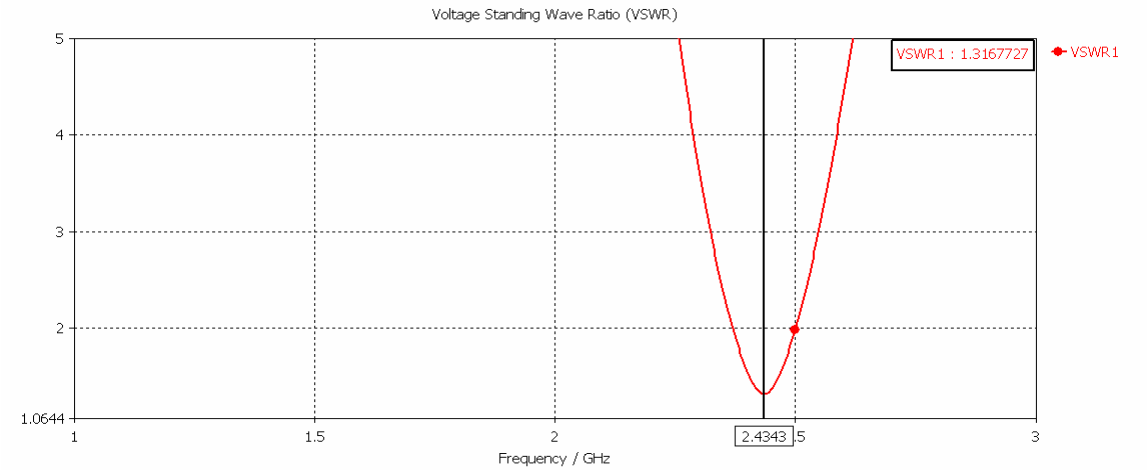

Figure 3.29: VSWR of the antenna.

The DGS is realized by etching a “defective” pattern in the ground plane, which disturbs the shield current distribution. This disturbance can change the characteristics of a transmission line, such as equivalent capacitance or inductance, to obtain and the band stop (“notch”) property. Figure 3.30 shows the current distribution of antenna.

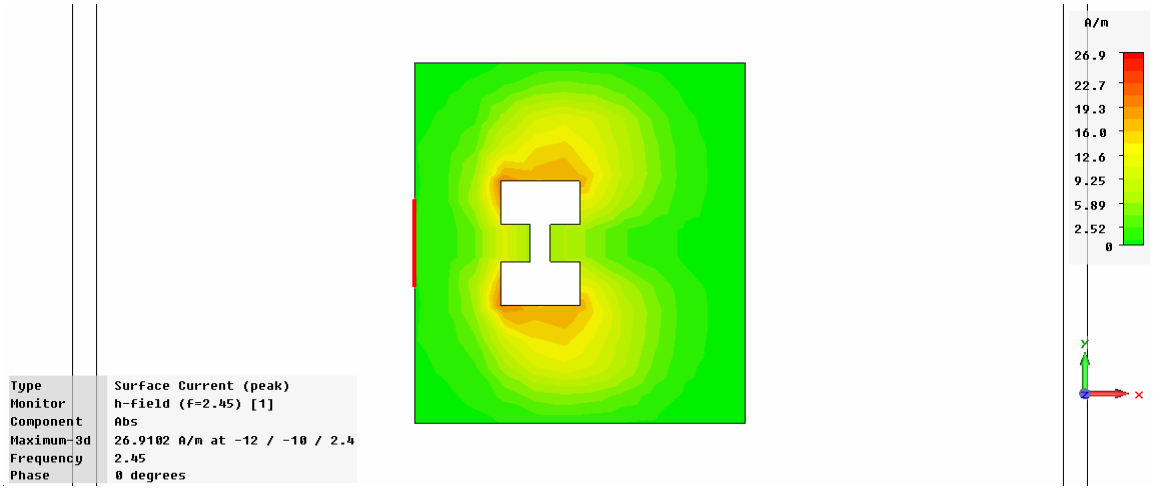

Figure 3.30: Surface current distribution of the antenna.

It is inferred from the figure 3.30 that the current lines have a much greater density at the arms of the dumbbell. A clearer view of the distribution is shown in figure 3.31.

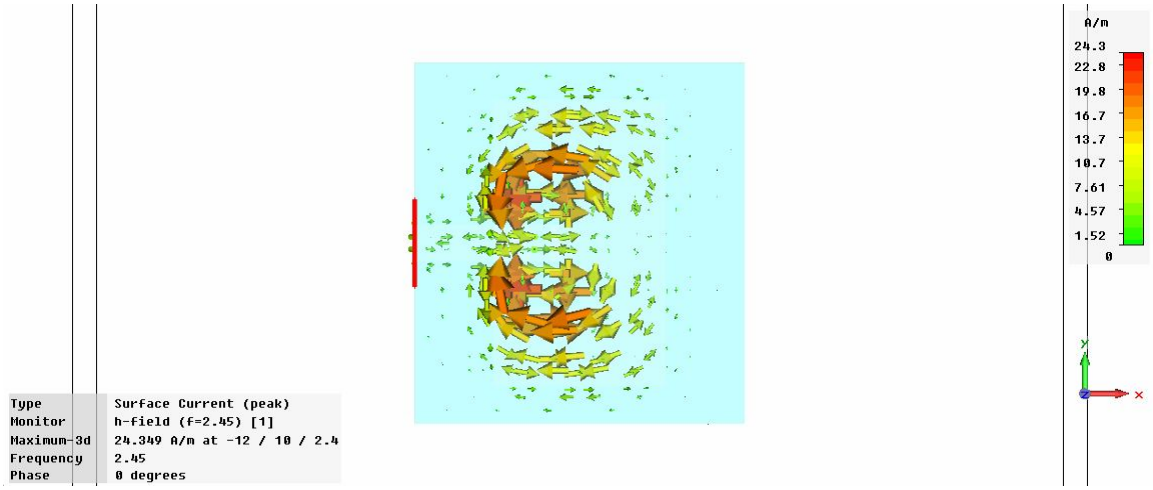

Figure 3.31: Current distribution at arms of dumbbell of the antenna

Thus, the antenna can be used for WLAN applications.

3.4.13 Summarized dimensional parameters

From the section 3.4, the values of various parameters are chosen for the optimized antenna. The selected parameters are summarized in form of table 3.10

Table 3.10 (Dimensions of the optimized antenna)

Parameter	L	W	L_f	W_f	L_{ap}	W_{ap}	L_s	Y_{os}	X_{os}	H
Dimension of Single band antenna(in mm)	25	46	23.5	6	30	3	4.5	6	0	2.4

3.5 Study of Antenna parameters

In this section the antenna parameters like directivity, gain, surface current etc are necessary to study in the desired bands so that the antenna can be used for the WLAN.

3.5.1 Directivity

The figure 3.32 shows that the directivity of the antenna increases with increase in the frequency.

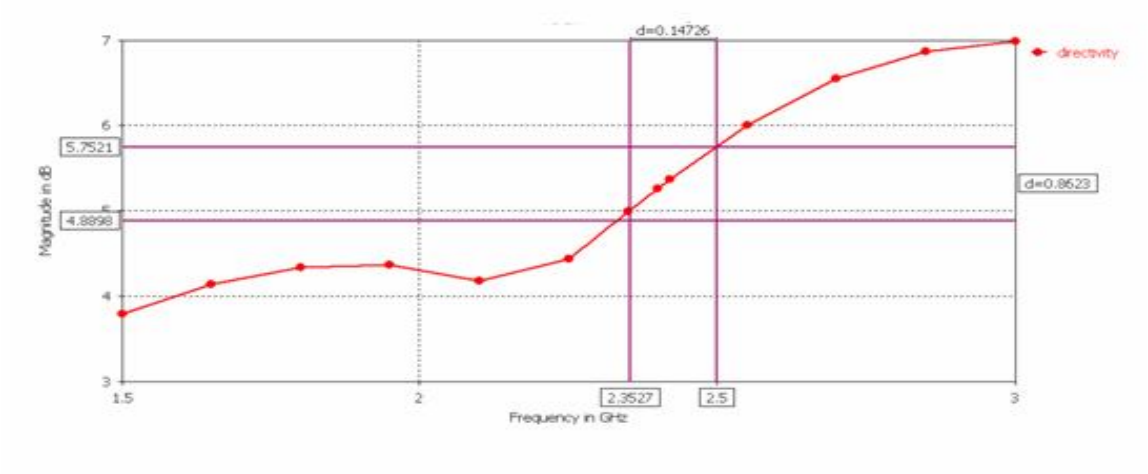

Figure 3.32: Directivity of the antenna.

In the desired band, the directivity varies from the 4.8898 dBi to 5.7521 dBi which is fair enough for WLAN application.

3.5.2 Gain

The figure 3.33 shows that the gain of the antenna increases with increase in the frequency

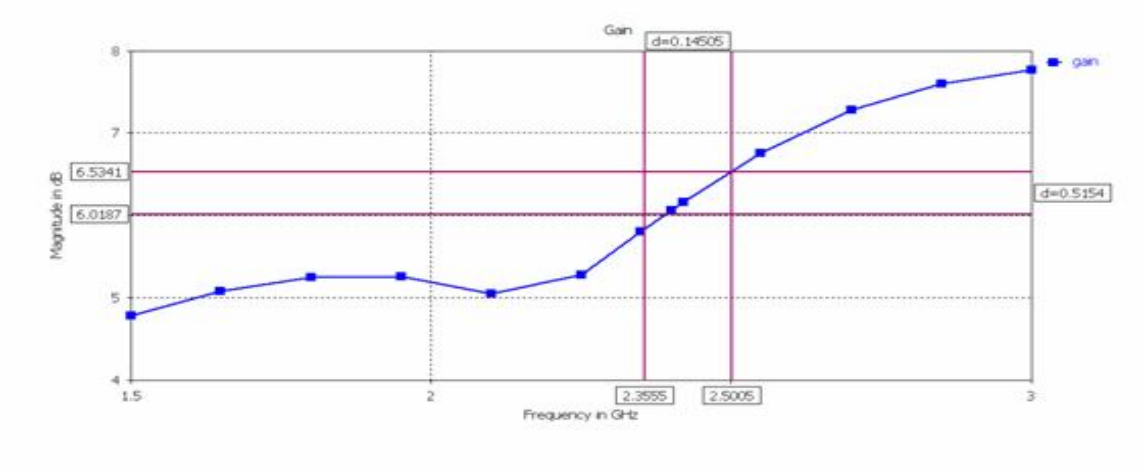

Figure 3.33: Gain of the antenna.

In the desired band, the gain varies from the 5.8 dB to 6.5341 dB which is fair enough for WLAN application. The figure 3.34 shows the absolute value of gain. The side lobe level is -2.8 dB with respect to the main lobe at a frequency of 2.42.

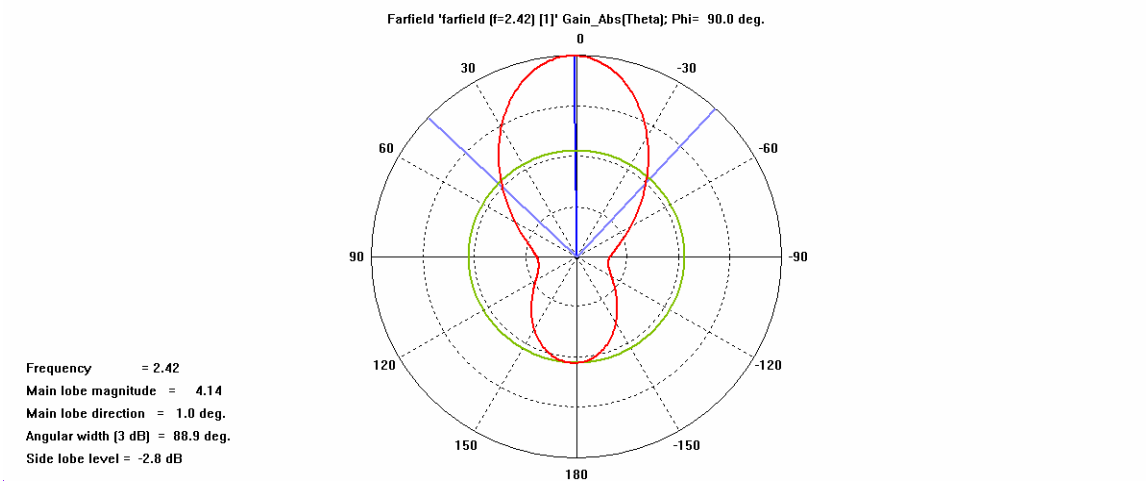

Figure 3.34: Polar plot of gain.

3.5.3 Surface current

The peak surface current at the frequency of 2.45 GHz is shown in the figure 3.35. The maximum surface current is obtained at the edges of the rectangular aperture in the ground is 31.1 A/m.

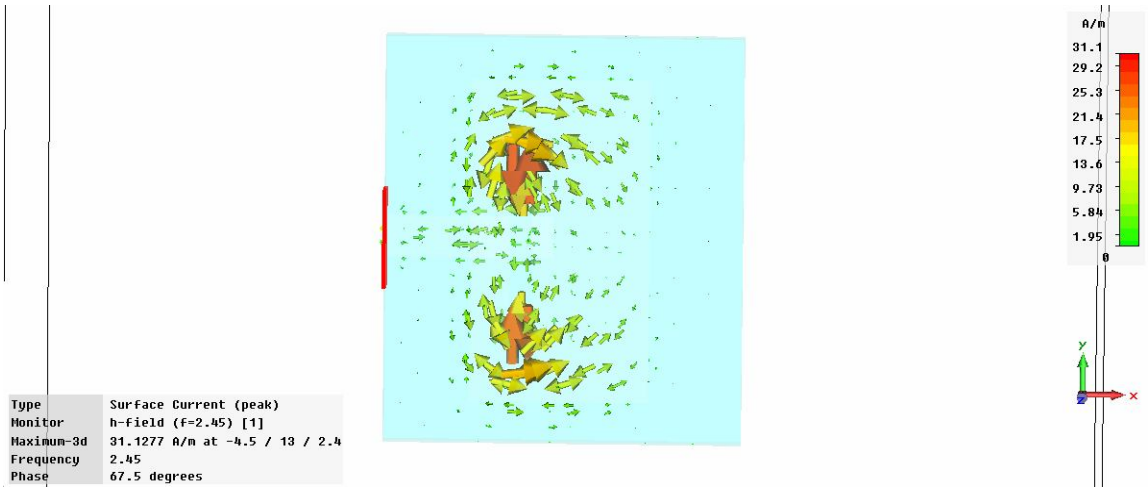

Figure 3.35: Surface current of the antenna

3.5.4 Broadband far-fields

The broadband directivity, gain, E-field, H-field and power field are important antenna parameters which a designer has to know about the antenna. Figure 3.36 shows the comparison of the far-fields calculated at a distance of 1 m from the antenna.

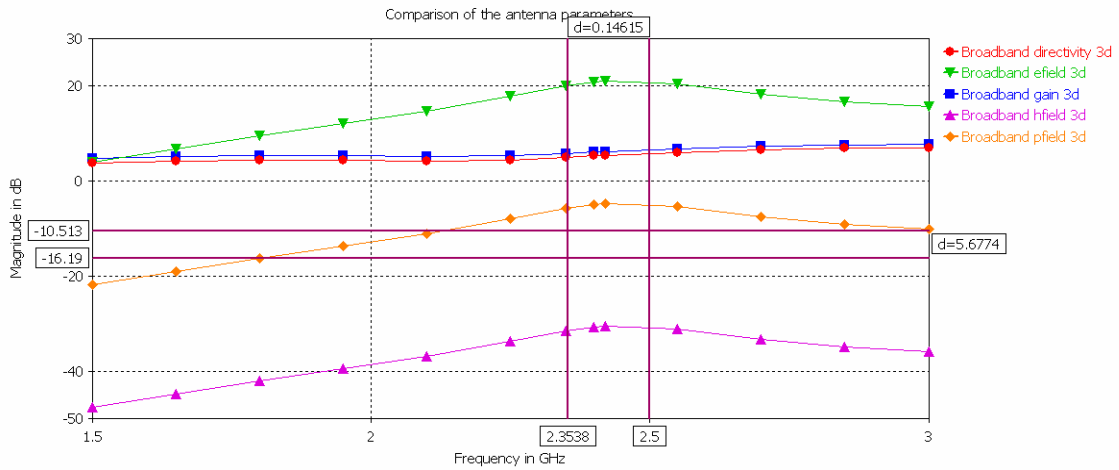

Figure 3.36: Broadband far-field radiation of the antenna.

The values of the antenna parameters at 2.42 GHz are summarized in the table 3.11.

Table 3.11(Antenna parameters for optimized antenna)

Parameter	Single Band
Frequency	2.42GHz

Directivity(dBi)	5.372
Gain(dB)	6.167
E-field(dBV/m)	20.93
H-field(dBA/m)	-30.59
Power(dBW/m^2)	-4.834

The antenna gives a percentage bandwidth 6.125 covering the band of 2.35 GHz-2.50 GHz. The antenna has a fair directivity and gain of 5.372 dBi and 6.167 dB respectively at frequency of 2.42 GHz. Thus, the antenna can be used for the WLAN applications.

Chapter 4

Dual band antenna design and its parametric study

With introduction of new wireless applications, operation at two or more discrete bands with an arbitrary separation of bands is desired. In such cases, a patch capable of operating in multiple bands is desirable. For most applications, all bands may be required to have the same polarization, radiation pattern, and bandwidth characteristics. Several methods of obtaining multi-bands or wide bands have been developed. Multi-banding of an antenna can be done by using E-shape, V-shape and U-shape patches patches [2],[6],[60]. One method is to use separate patches abreast each other for different applications. Stacking of the patches can also be used but it increases the volume of the antenna. An annular ring has also been used for dual frequency where the frequency for the propagating modes can be adjusted by choosing the inner and the outer radii. However, the ratio of the two frequencies is somewhat limited [39]. It is also possible to achieve dual frequency operation of a

patch antenna by loading slots at both the resonating side and at the non-resonating side of the patch and by using shorting pins [38-39]. It is also desirable to have one port and an arbitrary separation of the frequency bands. All of these requirements impose severe constraints on the use of natural modes [38-40].

4.1 Dual band antenna design

In chapter 3, an aperture coupled single band antenna for WLAN application was designed. Now, antenna is now loaded with two slots at the non-resonating side of the patch to make it to resonates at two frequency bands namely 2.18 GHz-2.20 GHz and 2.40 GHz-2.48 GHz for personal communication system (PCS) like smart homes and WLAN applications respectively. Figure 4.1 shows the two antennas for the desired applications.

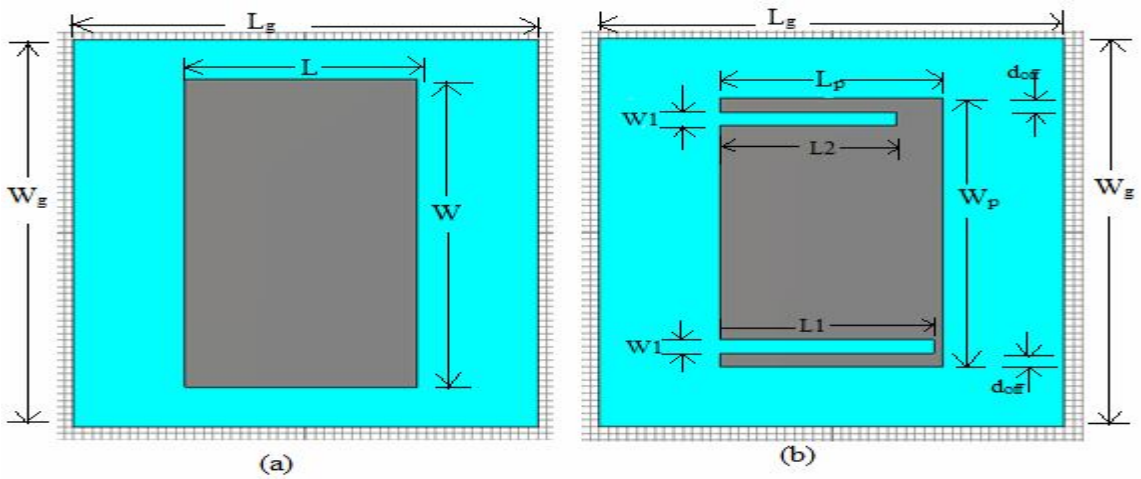

Figure 4.1: View of the a) Single band antenna b) Dual band antenna with slots

When the dual band antenna was excited by a Gaussian pulse at the waveguide port keeping all the parameters same as in case of the single band antenna, the S-parameter of the antenna is shown in the figure 4.2

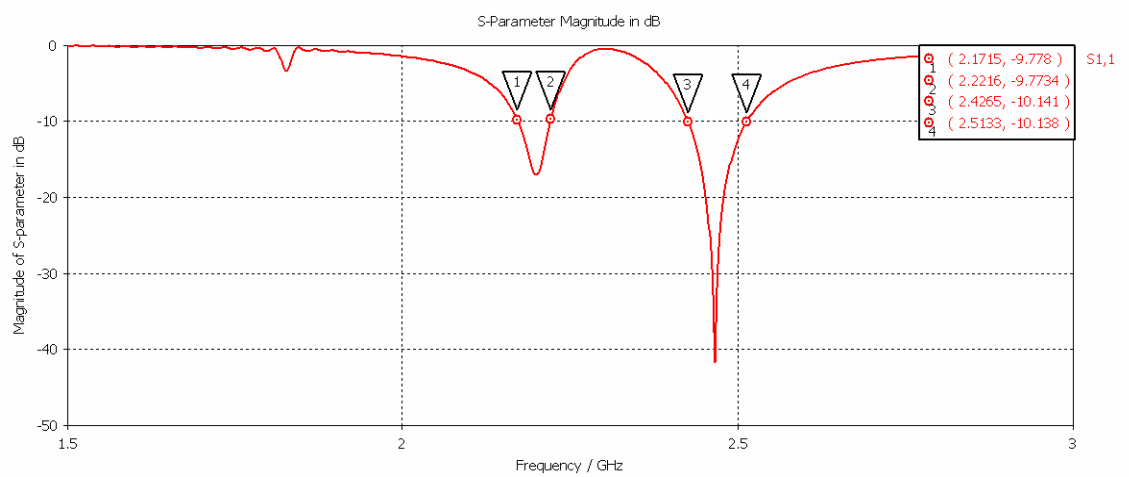

Figure 4.2: S-parameter of dual band antenna

From figure 4.2, it is revealed that the antenna covers a lower band of 2.1715GHz-2.2216GHz which is apt enough to be used for PCS and a higher band of 2.4265 GHz-2.5133GHz can be used for WLAN applications.

In figure 4.3, the Smith chart shows that the line impedance of the antenna is 74.86 ohm which can be easily matched with a 75 ohm SMA connector while testing the antenna.

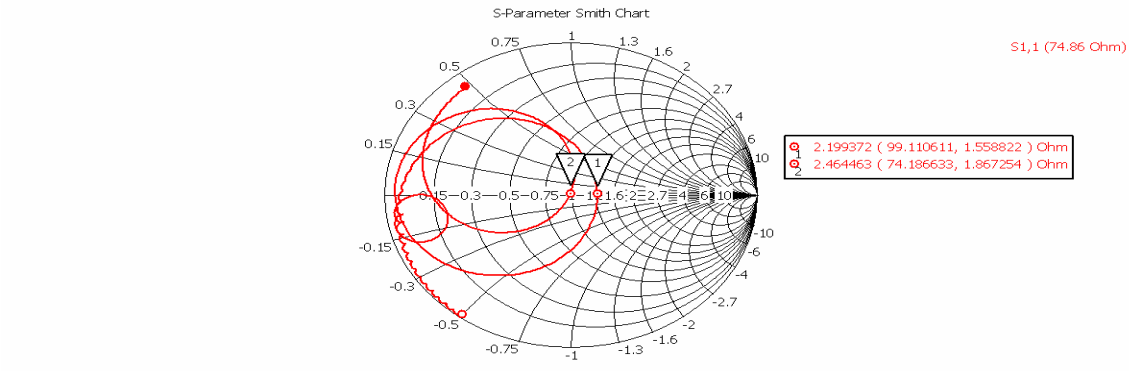

Figure 4.3: Smith chart of the dual band antenna.

It also depicts that the antenna resonates at 2.2 GHz and 2.466GHz for the dual band operation. It is consists of two circles apart from a very small circle where antenna seems to resonate at 1.76GHz but at this frequency the VSWR of the antenna is greater than 2,so it cannot be considered as the resonating frequency

4.2 Parametric study of the antenna

The parametric study of the proposed antenna is done using CST microwave studio. The effect of variation of different offsets and length is given below:

4.2.1 Effect of the change in the Offset (d_{off})

The variations in the resonating frequency with offset (d_{off}) is shown in figure 4.4. When the value of the offset is increased from 1mm to 4mm, there is a decrease in the resonant frequency and impedance matching of the antenna.

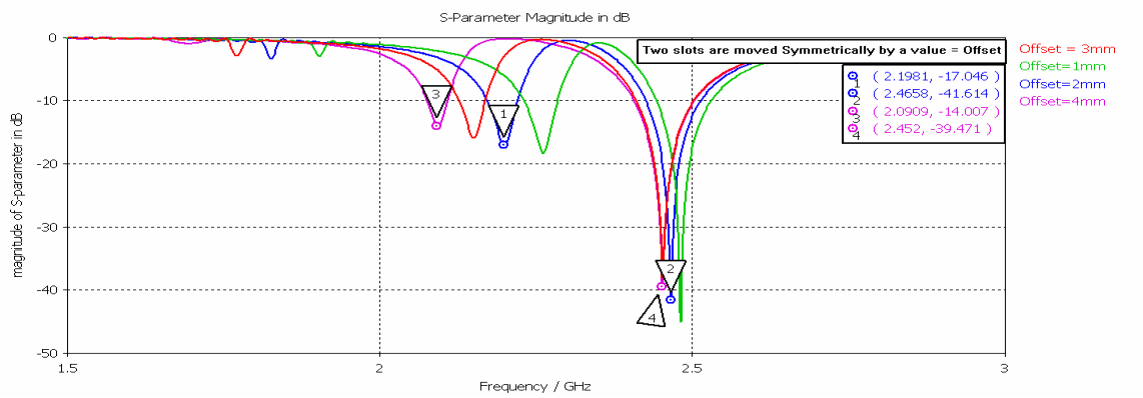

Figure 4.4: Variation of S-parameter with change in the Slot Offset (d_{off}).

The slots loaded have an optimum offset (d_{off}) equals to 2mm is chosen. The antenna parameters for the various offset values are tabulated in table 4.1.

Table 4.1 (Antenna parameters with varying Offset)

Parameters	Offset=1 mm		Offset=2 mm		Offset=3 mm		Offset=4 mm	
	F_r=2.2 GHz	F_r=2.45 GHz	F_r=2.2 GHz	F_r=2.45 GHz	F_r=2.2 GHz	F_r=2.45 GHz	F_r=2.2 GHz	F_r=2.45 GHz
Directivity (in dBi)	4.616	5.321	5.029	5.388	5.612	5.454	5.063	5.420
Gain(in dB)	5.458	6.148	5.845	6.215	6.357	6.272	4.935	6.227
E-Field (in dBV/m)	19.01	20.62	20.53	20.92	18.04	21.04	8.011	20.99
H-Fiel d(in dBA/m)	-32.51	-30.90	-30.99	-30.60	-33.48	-30.48	-43.51	-30.53
P-field (in dBW/m^2)	-6.753	-5.142	-5.233	-4.842	-7.717	-4.723	-17.75	-4.767

4.2.2 Effect of change in the length (L2) of slot 2 keeping the length (L1) of slot 1 constant

The slot length also affects the resonating frequency and bandwidth of the antenna. Figure 4.5 show the variation of resonant frequency and bandwidth of antenna when length (L2) of slot 2 is varied from 7 mm to11mm keeping the length (L1) of the slot1 is fixed at 11 mm. With increase in the length L2, there is decrease in matching characteristics but increase in the bandwidth of the antenna. The resonating frequency of the both the bands decrease with the increase in the length of slot 2. Also, there is a significant shift in the resonant frequency of the lower band as compared to the higher band, showing that the slot 2 is responsible for resonating at low frequencies.

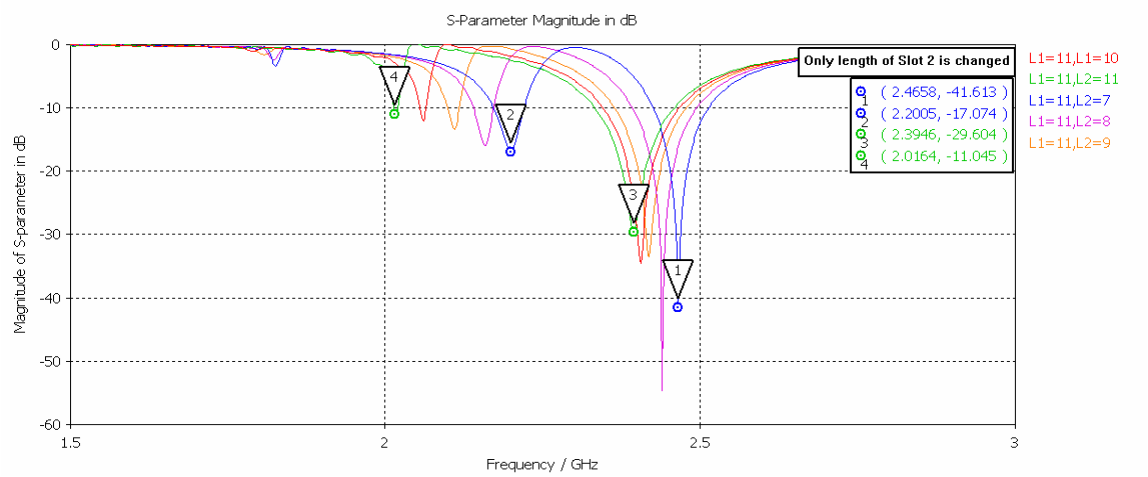

Figure 4.5: Variation of S-parameter with change in length of slot2.

From the figure 4.5, the length L2 equals to 7 mm is chosen as it gives us the desirable bands at 2.2005 GHz and 2.4658 GHz. The antenna parameters for variable length L2 are tabulated in table 4.2

Table 4.2 (Antenna parameters with varying L2)

Parameters	L2=7mm		L2=8mm		L2=9mm		L2=10mm		L2=11mm	
	F_r=2.2GHz	F_r=2.45GHz	F_r=2.2GHz	F_r=2.45GHz	F_r=2.2GHz	F_r=2.45GHz	F_r=2.2GHz	F_r=2.45GHz	F_r=2.2GHz	F_r=2.45GHz
Directivity (in dBi)	5.029	5.388	5.763	5.461	3.989	5.23	4.021	5.551	4.054	5.580
Gain(in dB)	5.845	6.215	6.488	6.270	4.804	6.331	4.735	6.349	4.877	6.366
E-Field(in dBV/m)	20.53	20.92	17.04	21.02	11.45	20.97	14.95	20.88	16.11	20.79

H-Field(in dBA/m)	-30.99	-30.60	-34.49	-30.50	-40.07	-30.55	-36.57	-30.64	-35.41	-30.73
P field(in dBW/ m^2)	-5.233	-4.842	-8.725	-4.737	-14.31	-4.793	-10.81	-4.882	-9.653	-4.971

Figure 4.6 reveals that surface current at 2.2 GHz is highest near the slot 2 proving that slot 2 is responsible for the resonating at the lower frequency band. The maximum value of the surface current is 69.2 A/m.

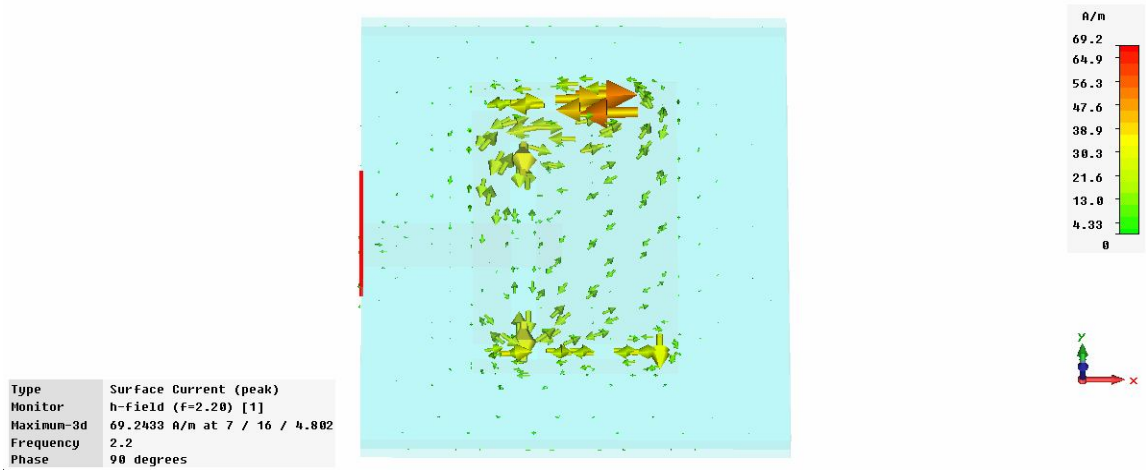

Figure 4.6: Surface current of the antenna at 2.2 GHz.

4.2.3 Effect of change in the length (L1) of slot 1 keeping the length (L2) of slot2 constant

The variation of resonant frequency and impedance characteristics with length (L1) is shown in figure 4.7. The length (L1) of slot 1 is varied from 7mm to 11mm keeping the length L2 of slot 2 at 7mm. With increase in slot length L1 the resonant frequency decreases. It is observed from the figure 4.7 that the higher band frequency subjects to a much greater change due to increase in length of slot 1 as compared to lower frequency band.

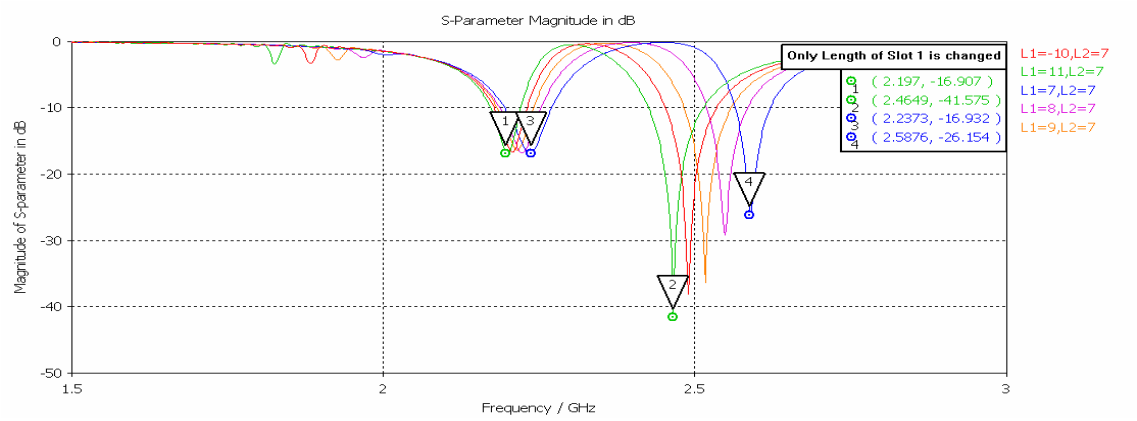

Figure 4.7:- Variation of S-parameter with change in length of slot1.

The length L1 equals to 11 mm is chosen as it gives the optimum results for the desired application. The antenna parameters variable length L1 studied are tabulated in table 4.3

Table 4.3 (Antenna parameters with varying L1)

Parameters	L1=7mm		L1=8mm		L1=9mm		L1=10mm		L1=11mm	
	F_r=2.2 GHz	F_r=2.45 GHz	F_r=2.2 GHz	F_r=2.45 GHz	F_r=2.2 GHz	F_r=2.45 GHz	F_r=2.2 GHz	F_r=2.45 GHz	F_r=2.2 GHz	F_r=2.45 GHz
Directivity(in dBi)	4.730	2.993	4.789	3.940	4.842	4.874	4.922	5.213	5.029	5.388
Gain(in dB)	5.556	3.535	5.619	4.833	5.661	5.733	5.737	6.054	5.845	6.215
E-Field (in dBV/m)	19.94	3.720	20.13	13.07	20.23	18.45	20.38	20.27	20.53	20.92
H-Field (in dBA/m)	-31.58	-47.80	-31.39	-38.45	-31.29	-33.07	-31.14	-31.25	-30.99	-30.60
P-Field (in dBW/m^2)	-5.824	-22.04	-5.632	-12.69	-5.526	-7.306	-5.380	-5.488	-5.233	-4.842

Figure 4.8 shows the surface current of the antenna at 2.45 GHz. The slot 1 is responsible for radiations at the higher frequency band as the current due to slot 2 seems to be cancelled by oppositely flowing current. The maximum surface current at 2.45 GHz is 47.284 A/m.

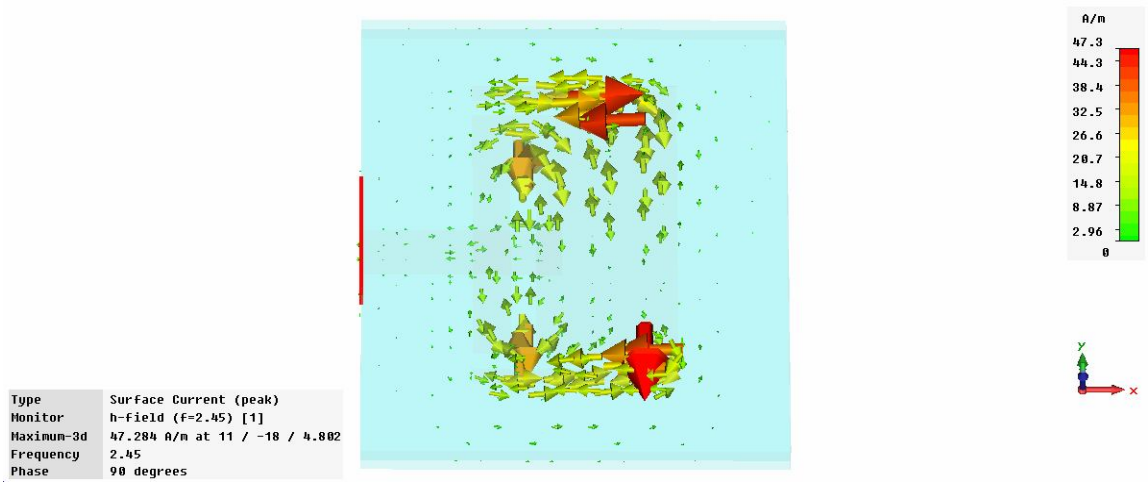

Figure 4.8: Surface current of the antenna at 2.45 GHz.

4.2.4 Effect of change in the Slot Widths

The variation of resonant frequency with the slot width (W1) from 1mm to 4mm symmetrically for both the slots is shown in figure 4.9. By increasing slot width from 1mm to 4 mm, decreases the resonating frequency and the coupling level.

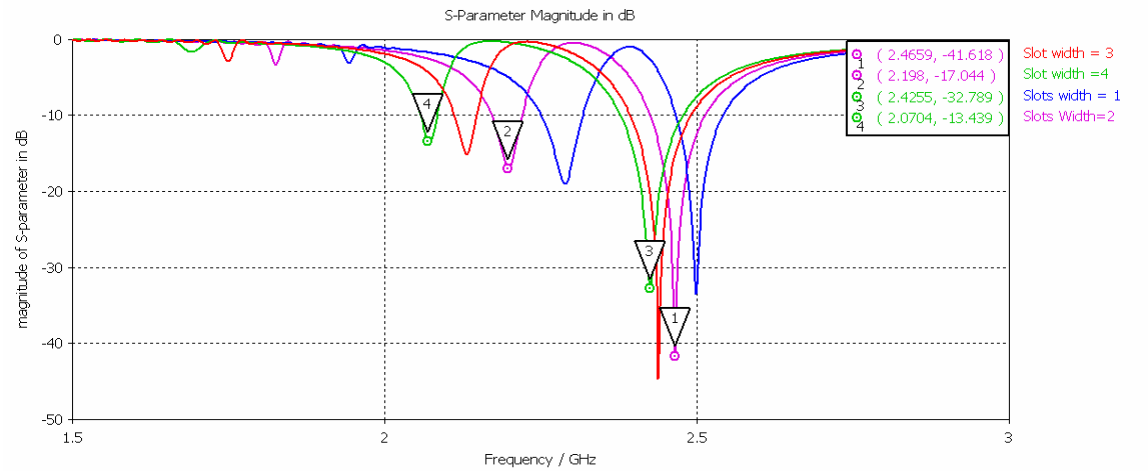

Figure 4.9: Variation of S-parameter with change in width of the two slots symmetrically.

The value of slot width equals to 2 mm is chosen corresponding to which the antenna covers the frequency bands of 2.2 GHz and 2.46 GHz.

4.3 Comparison of Single and Dual band antenna

In chapter 3, single band antenna is designed for WLAN application. In this chapter, the dual band antenna is designed. Figure 4.10 shows comparison of the two antennas in terms of S-parameter.

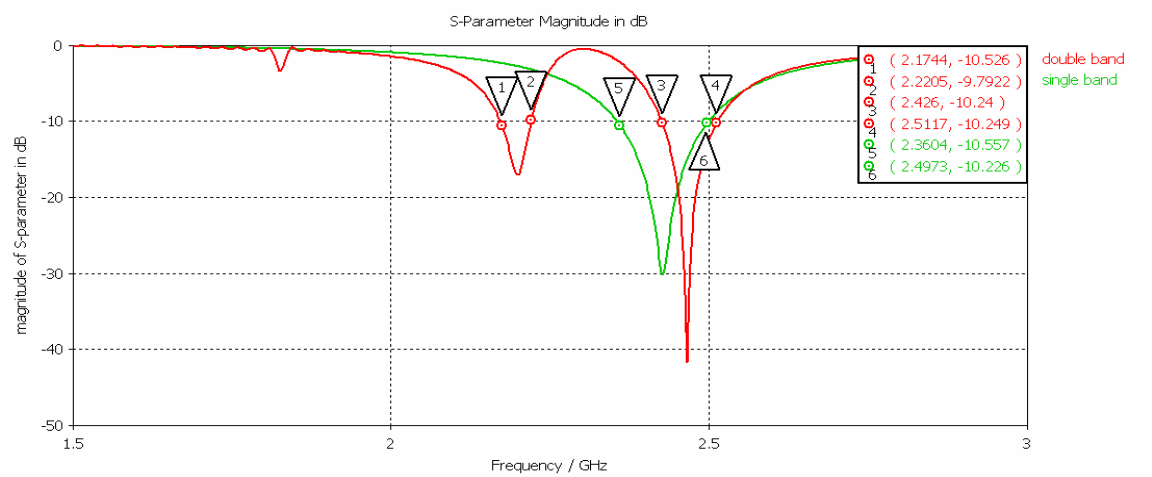

Figure 4.10: S-parameter of the two antennas.

For the single band antenna, it can be inferred that, it resonates in the range 2.3603 GHz-2.4973 GHz, giving us a 10 dB bandwidth of 137 MHz which covers the WLAN standard 2.40-2.48 GHz. The minimum return loss is obtained at the resonating frequency 2.4284 GHz is -30.063 dB. For the dual band antenna, there are two bands covering the ranges 2.18 GHz-2.20 GHz and the 2.40 GHz- 2.48 GHz. The bandwidth of the antenna at the lower and the higher bands is 46MHz and 85 MHz respectively. Also, the minimum return loss of the antenna at lower and higher bands is -16.907 dB and -41 dB respectively. Figure 4.11 shows the Smith chart of the two antennas.

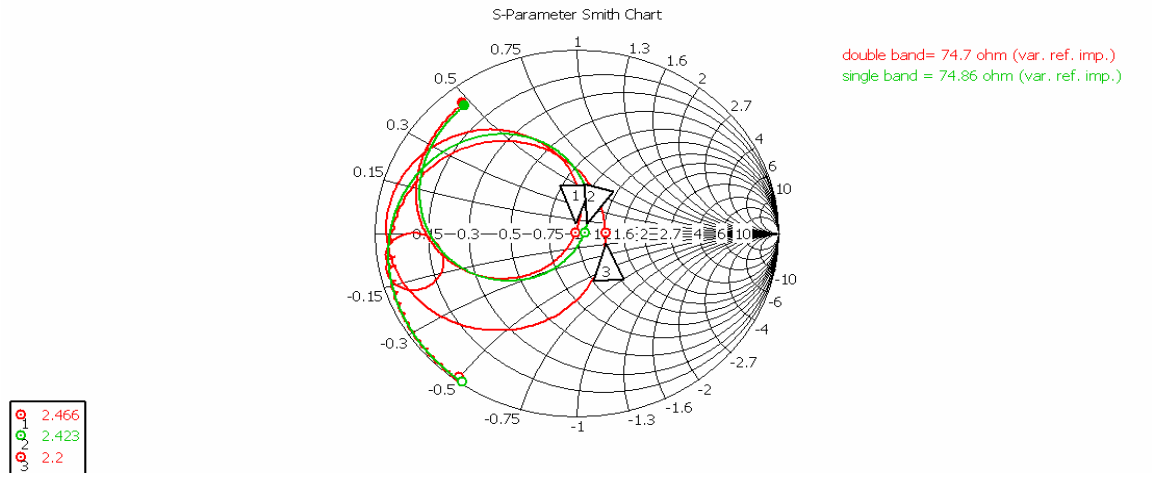

Figure 4.11: Smith chart of two antennas.

The figure 4.11 shows the Smith chart of the two antennas. The line impedance of the antenna is 74.86 ohm which can be easily matched with a 75 ohm SMA connector while testing the antenna. The Smith chart of the antenna shows the antenna resonates at 2.423GHz for single and 2.2 GHz and 2.466 GHz for the double band

operation. It can also be inferred that the single band antenna have only one resistance circle and the double band has two apart from a very small circle where antenna seems to resonate at 1.76GHz but at this frequency the VSWR of the antenna is greater than 2,so it cannot be considered as the resonating frequency. The comparison of antenna parameters for both the antennas is listed in the Table 4.4.

Table 4.4 (Comparison of antenna parameters for designed the antennas)

Parameters	Single Band	Double Band	
Frequency	2.42 GHz	2.20 GHz	2.45 GHz
Directivity(dBi)	5.372	5.033	5.402
Gain(dB)	6.167	5.849	6.229
E-field(dBV/m)	20.93	20.53	20.93
H-field(dBA/m)	-30.59	-30.99	-30.59
Power(dBW/m^2)	-4.834	-4.828	-4.828

The directivity of the antennas is above 5dBi in each case, makes it suitable for the wireless applications. They have an appreciable gain of around 6 dB. The E-field, H-field and the Power measured at a distance of 1metre are also listed. The table 4.4 shows that the directivity of the antenna at 2.20GHz and 2.46GHz as 5.033dBi and 5.402dBi, and gain as 5.849dB and 6.0229dB respectively. These values are fair enough to be used for the PCS and WLAN applications.

4.4 Fabrication of the antenna

The hardware design of the antenna includes two processes namely PCB (Printed circuit board) design and testing of the antenna. The various steps for the PCB design are explained as:

1) Drafting of the layers on transparent sheet: - Firstly all layers of the antenna to be designed are drafted on a transparent sheet whose photo is taken by the camera on a film containing silver bromide coating in a dark room. If the dimensions are very small, then the scaled diagram of the layers can be drawn and the camera settings are changed accordingly. Figure 4.12 shows the layers drafted on a transparent sheet.

2) Negative developing: - The film with silver coating is washed in A+B solution for not more than 2-3 minutes otherwise the whole film will become black. Then, the film is washed in the negative developer and dried at a temperature up to 50-60°C. Now, the negative of the layers is obtained and can be taken to sunlight. Figure 4.13 and 4.14 shows the negatives of the different layers.

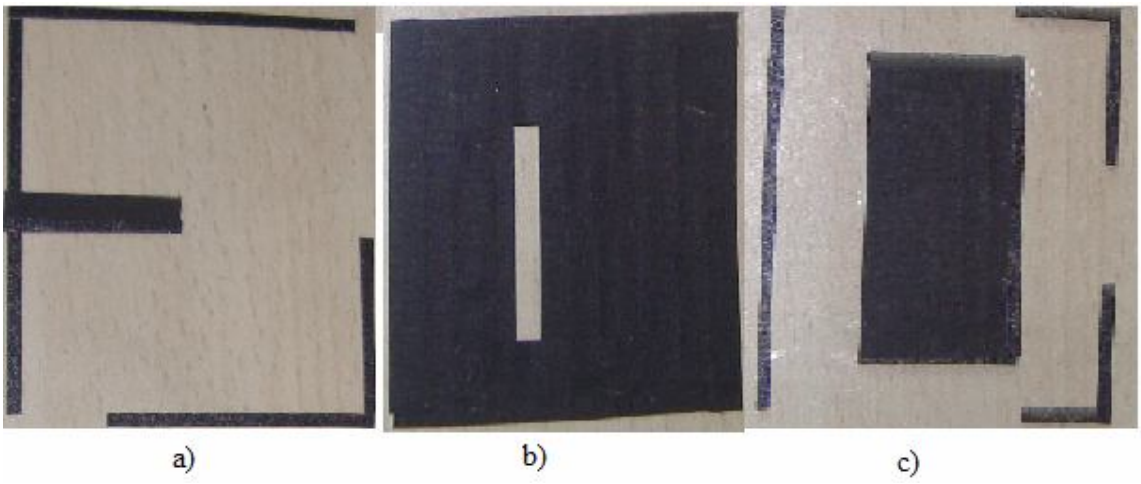

Figure 4.12: Layer drafted on transparent sheet a) Feedline b) Aperture in ground c) Patch of single band antenna.

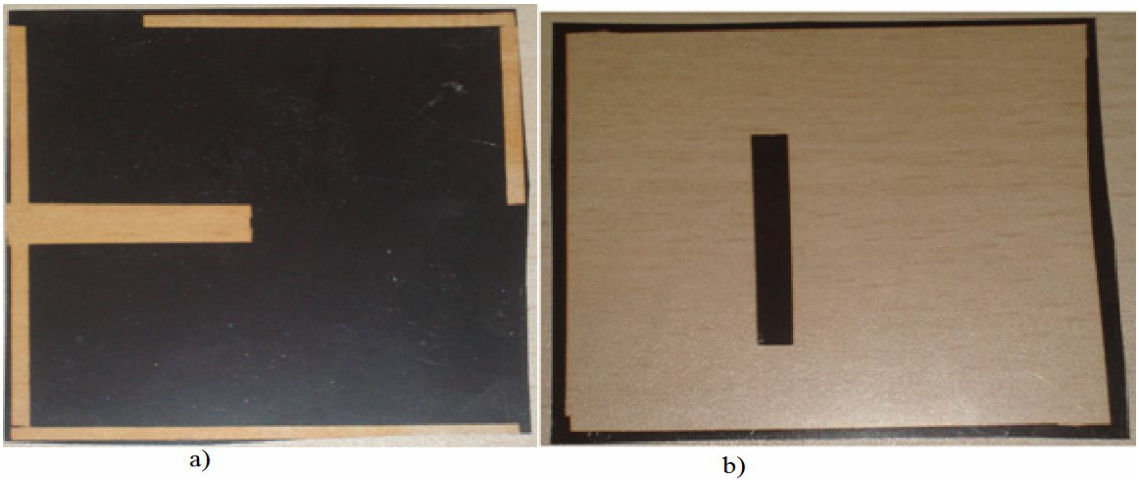

Figure 4.13: Negatives of a) Feedline b) Aperture in ground slot.

3) Operations on PCB: - The PCB is cleaned with a brush and cut in the desired size. Now the PCB is dipped once in the photo resist developer placed in yellow light. It dried in an oven for 3-5 minutes. Now the negatives are put on the PCB with proper alignment and exposed to ultraviolet radiations for 3

minutes. The PCB is washed carefully with photo resist developer in a well cleaned container and etching is done with $FeCl_3$. The designed PCB is shown in the figure 4.15.

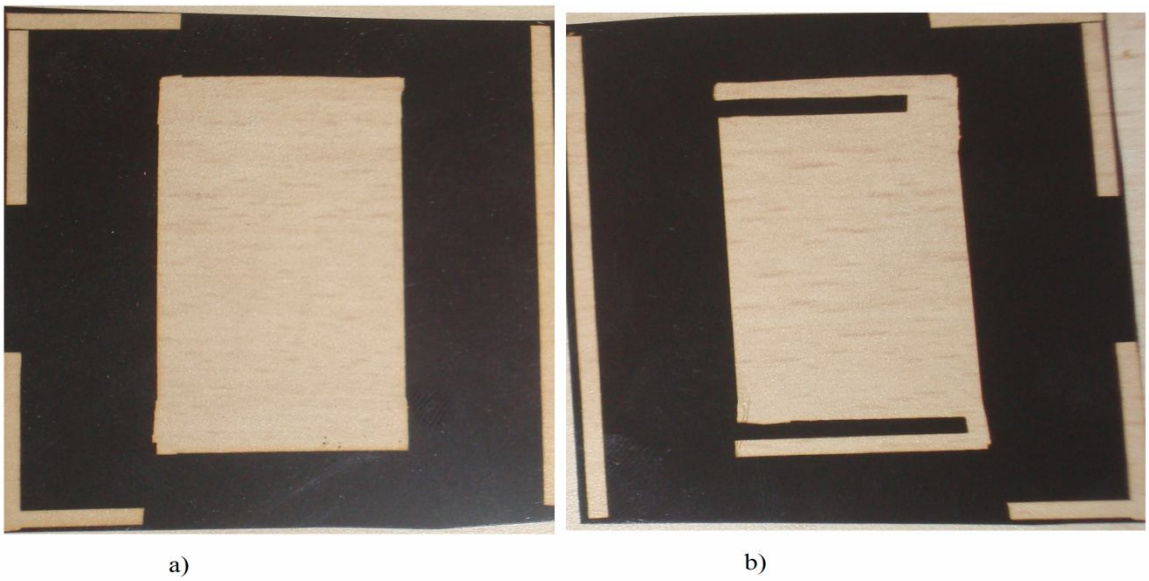

Figure 4.14: Negatives of Patches of a) Single band antenna b) Double band antenna.

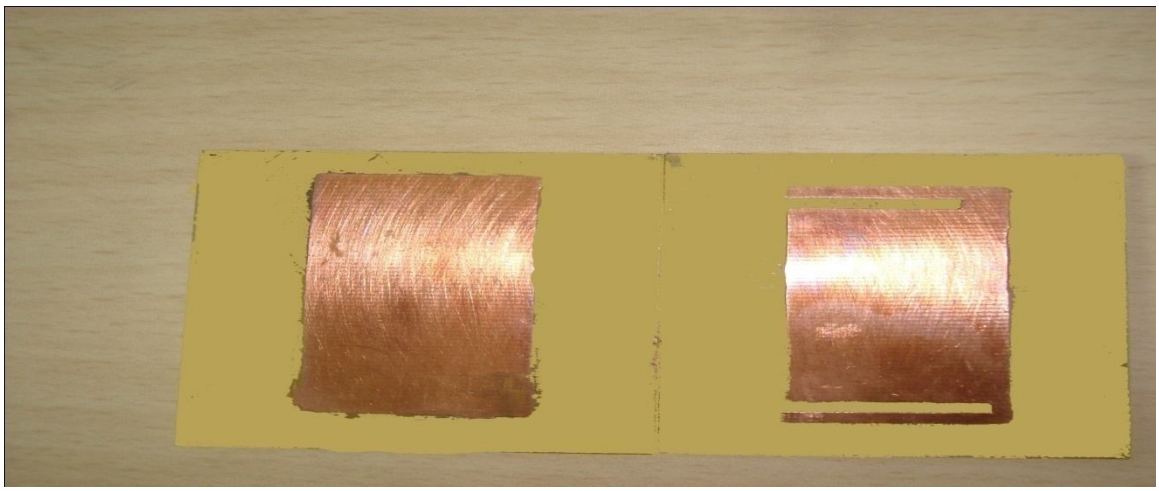

Figure 4.15: Patches of a) Single b) Double band antenna.

Figure 4.16: Fabricate flow of the PCB design.

The steps for antenna fabrication are shown via a flowchart drawn in the figure 4.16. The two fabricated PCBs are joined with adhesive and a SMA connector is soldered at the feed point and the antenna is ready for the testing.

Chapter 5

Conclusion and Future Work

5.1 Conclusion

In this report, firstly an aperture coupled, rectangular patch single band antenna was designed which resonates at 2.43 GHz and provides a bandwidth of 142 MHz, hence, this antenna can be used for the WLAN applications. The designed antenna provides a percentage bandwidth 5.84. The physical parameters examined in this study include the dimensions and locations of the substrates and their dielectric constants, feed line, ground plane coupling slot, and patch. The antenna parameters like operating frequency, input impedance, VSWR, Bandwidth, Return loss, directivity and gain are determined for each antenna configuration. Also, the effect of the physical parameters is studied on the antenna parameters.

The designed antenna is loaded with two appropriately positioned and dimensioned slots at the non-resonating sides of the patch making it to dual band resonating at 2.20 GHz and 2.45 GHz. The percentage bandwidth of the dual band antenna at 2.20 GHz and 2.45 GHz is 2.27and 3.67 respectively. The directivity and gain of the antenna are fair enough to be used for the personal communication system and WLAN applications.

5.2 Future Work

The research work could be extended to

- Multibanding of the antenna for various wireless applications.
- Array designing to enhance the gain and other antenna properties.
- Optimization of the antenna using Genetic algorithm, Neural network, PSO (Particle Swarm optimization).
- The antenna could be easily fabricated and tested for the desired results.

List of publication

- Ved Prakash, Dr. Rajesh Khanna, "Aperture Coupled Microstrip Antenna For WLAN Applications" , SPIN conference, Feb 23-24, 2011,

Communicated:

- Ved Prakash, Dr. Rajesh Khanna, "Dual Band Aperture Coupled Rectangular Patch Antenna For PCS and WLAN Applications", to International of Communication Engineering Applications, to be published in July 2011.

References

[1] G. A. Deschamps, “Microstrip microwave antennas”, 3rd USAF Symposium on Antennas, 1953.

[2] I. J. Bahl and P. Bhartia, Microstrip Antennas, Artech House, 1980.

[3] James, J. R., and P. S. Hall, Handbook of Microstrip Antennas, Vol. 1, London: Peter Peregrinus Ltd., 1989.

[4] Lee, H. F., and W. Chen, Advances in Microstrip and Printed Antennas, New York: John Wiley & Sons, 1997.

[5] G. Kumar and K. P. Ray, Broadband Microstrip Antennas, Artech House, 2003.

[6] C. A. Balanis, Antenna Theory, 3rd ed. John Wiley & Sons, Hoboken, NJ, 2005.

[7] Waterhouse, Microstrip Patch Antennas, World scientific publication house co.pte.ltd, 2003.

[8] Bhatacharya, A. K., and R. Garg, ‘‘Generalized Transmission Line Model for Microstrip Patches,” IEE Proc. Microwaves, Antennas Propagation, Pt. H, Vol. 132, No. 2, pp. 93–98, 1985.

[9] Dubost, G., and G. Beauquet, ‘‘Linear Transmission Line Model Analysis of a Circular Patch Antenna,” Electronics Letters, Vol. 22, pp. 1174–1176, October 1986.

[10] Babu, S., I. Singh, and G. Kumar, ‘‘Improved Linear Transmission Line Model for Rectangular, Circular and Triangular Microstrip Antennas,’’ IEEE AP-S Int. Symp. Digest, pp. 614–617, July 1997.

[11] Lo, Y. T., D. Solomon, and W. F. Richards, ‘‘Theory and Experiment on Microstrip Antennas,” IEEE Trans. Antennas Propagation, Vol. AP-27, pp. 137–145, March 1979.

[12] Richards, W. F., Y. T. Lo, and D. D. Harrison, ‘‘An Improved Theory for Microstrip

Antennas and Applications,” IEEE Trans. Antennas Propagation, Vol. AP-29, pp. 38–46 January 1981.

[13] Lo, T., and S. W. Lee, Antenna Handbook, New York: Van Nostrand Reinhold, 1988

[14] Kane Yee, "Numerical solution of initial boundary value problems involving Maxwell's equations in isotropic media". IEEE Transactions on Antennas and Propagation”, 302–307, 1966.

[15] A. Taflove ,"Application of the finite-difference time-domain method to sinusoidal steady state electromagnetic penetration problems". IEEE Transactions on Electromagnetic Compatibility, 191–202, 1980.

[16] Lee, H. F., and W. Chen, Advances in Microstrip and Printed Antennas, New York: John Wiley & Sons, 1997.

[17]http://en.wikipedia.org/wiki/Finite-difference_time-domain_method last accessed on June 15,2011.

[18]http://photonics.tfp.unikarlsruhe.de/fileadmin/conferences/heraeus386/Heraeus386_Lavrinenko. pdf last accessed on June 15, 2011.

[19] D. M. Pozar, "A Microstrip Antenna Aperture Coupled to a Microstrip Line", Electronics Letters, Vol. 21, pp.49-50, January 17, 1985.

[20] D. M. Pozar, "Microstrip antennas", IEEE Proc., vol. 80, pp. 79-91, January 1992.

[21] D. H. Schaubert, "Microstrip antennas", Electromagnetics, vol. 12, pp. 381-401, 1992.

[22] D. M. Pozar, "A Review of Aperture Coupled Microstrip Antennas: History, Operation, Development, and Applications", 1996

[23] D. M. Pozar and D. H. Schaubert, Microstrip Antennas: The analysis and design of microstrip antennas and arrays, IEEE Press, New York, 1995.

[24] Y. Yoshimura, "A microstripline slot antenna", IEEE Trans. Microwave Theory and Techniques, vol. MTT-20, pp. 760-762, November 1972.

[25] J.-F. Zurcher, "The SSFIP: A global concept for high performance broadband planar antennas", Electronics Letters, vol. 24, pp. 1433-1435, November 1988.

[26] S. Targonski and D. M. Pozar, "Design of wideband circularly polarized aperture coupled microstrip antennas", IEEE Trans. Antennas and Propagation, vol. 41, pp. 214-220, February 1993.

[27] F. Croq and A. Papiernik, "Large bandwidth aperture coupled microstrip antenna", Electronics Letters, vol. 26, pp. 1293-1294, August 1990.

[28] F. Croq and A. Papiernik, "Stacked slot-coupled printed antenna", IEEE Microwave and Guided Wave Letters, vol. 1, pp. 288-290, October 1991.

[29] F. Croq and D. M. Pozar, "Millimeter wave design of wide-band aperture coupled stacked microstrip antennas", IEEE Trans. Antennas and Propagation, vol. 39, pp. 1770-1776, December 1991.

[30] M. Edimo, P. Rigoland, and C. Terret, “Wideband dual polarized aperture coupled stacked patch antenna array operating in C-band”, Electronics Letters, vol. 30, pp. 1196-1197, July 1994.

[31] S. D. Targonski and R. B. Waterhouse, “An aperture coupled stacked patch antenna with 50% bandwidth”, IEEE International Symposium on Antennas and Propagation, Baltimore, MD. 1996.

[32] H.S. Shin and N. Kim “Wideband and high-gain one-patch microstrip antenna coupled with H-shaped aperture” Electronics Letters, Vol. 38 No.19, 12th September 2002.

[33] R. Joseph and T. Fukusako, “Bandwidth enhancement of circularly polarized square slot antenna” Progress In Electromagnetics Research B, Vol. 29, 233-250, 2011.

[34] B. Vedaprabhu and K. J. Vinoy, “ An Integrated wideband multifunctional antenna using a microstrip patch with two U-slots” Progress In Electromagnetics Research B, Vol. 22, 221-235, 2010

[35] C.-J. Wang and S.-W. Chang, “Studies on dual-band Multi-slot antennas” Progress In Electromagnetics Research, PIER 83, 293–306, 2008

[36] S. Maci and G. BifJi Gentili, “ Dual-Frequency Patch Antennas” IEEE Antennas and Propagation Magazine, Vol. 39, No. 6, December 1997.

[37] J. C. Liu,B. H. Zeng, C. Y. Liu, H. C. Wu and C. C. Chang, “ A dual-mode Aperture-coupled Stack antenna for WLAN dual-band and circular polarization applications, Progress In Electromagnetics Research C, Vol. 17, 193-202, 2010.

[38] Wang,B.F., and Y.T.Lo, “Microstrip Antennas for Dual Frequency Operation”,IEEE trans. Antennas and Propagation,Vol. AP-32., pp 938-943, 1984.

[39] Yazidi, M.El, M.Himdi, and J.P. Daniel,” Aperture Coupled Microstrip Antennas for Dual Frequency operation,” Electron. Lett. , Vol-29,pp. 1506-1508, 1993

[40] Lu, J.-H, “Single feed Dual frequency rectangular microstrip Antenna with pair of step-slots,” Electron.Lett. , vol.35,, pp. 354-355. 1999.

[41] Rashid A. Saeed, S. Khatun, Borhanuddin, M. A. Khazani, Rania A. Mokhtar and Mahmoud Alshamary, “ Design of Single Fed Aperture Coupled Microstrip Antennas for WLAN” IEEE, 2005

[42] O. Tze-Meng and T. K. Geok, “ A dual-band Omni-directional microstrip antenna” Progress In Electromagnetics Research, Vol. 106, 363–376, 2010.

[43] Y.-C. Lee and J.-S. Sun, " Compact Printed slot antennas for Wireless Dual and Multi-band operations" Progress In Electromagnetics Research, PIER 88, 289–305, 2008

[44] C. Mahatthanajatuphat, S. Saleekaw, and P. Akkaraekthalin and M. Krairiksh, " A Rhombic patch Monopole antenna with modified Minkowski fractal geometry for UMTS, WLAN, and MOBILE WIMAX application" Progress In Electromagnetics Research, PIER 89, 57–74, 2009

[45] C. Mahatthanajatuphat and P. Akkaraekthalin and S. Saleekaw, "A Bidirectional Multiband antenna with modified Fractal slot fed by CPW" Progress In Electromagnetics Research, PIER 95, 59-72, 2009.

[46] R. S. Aziz, M. A. S. Alkanhal, and A. F. A. Sheta, "Multiband fractal-like antennas" Progress In Electromagnetics Research B, Vol. 29, 339-354, 2011.

[47] F. Bilotti and C. Vegni, " Design of Polygonal patch antennas for portable devices" Progress In Electromagnetics Research B, Vol. 24, 33-47, 2010.

[48] P. L. Sullivan and D. H. Schaubert, "Analysis of an aperture coupled microstrip antenna", IEEE Trans. Antennas and Propagation, vol. AP-34, pp. 977-984, August 1986.

[49] D. M. Pozar, "A reciprocity method of analysis for printed slot and slot coupled microstrip antennas", IEEE Trans. Antennas and Propagation, vol. AP-34, pp. 1439-1446, December 1986

[50] M. Himdi, J. P. Daniel, and C. Terret, "Analysis of aperture coupled microstrip antenna using cavity method", Electronics Letters, vol. 25, pp. 391-392, March 1989.

[51] M. El Yazidi, M. Himdi, and J. P. Daniel, "Transmission line analysis of non-linear analysis of slot coupled microstrip antenna", Electronics Letters, vol. 28, pp. 1406-1407, July 1992

[52] D. Yau and N. V. Shuley, "Numerical analysis of an Aperture Coupled Microstrip Patch antenna using Mixed Potential Integral equations and complex images" Progress In Electromagnetics Research, PIER 18, 229–244, 1998.

[53] S.-Q. Xiao, Z. H. Shao, and B.-Z. Wang, " Application of the improved Matrix type FDTD method for active antenna analysis" Progress In Electromagnetics Research, PIER 100, 245-263, 2010.

[54] J. Li, L.-X. Guo, and H. Zeng, "FDTD method investigation on the polarimetric scattering from 2-d rough surface" Progress In Electromagnetics Research, PIER 101, 173-188, 2010.

[55] Y.-H. Liu and Q. H. Liu and Z.-P. Nie, “ A new efficient FDTD time-to-frequency domain conversion algorithm” Progress In Electromagnetics Research, PIER 92, 33–46, 2009.

[56] J. P. Geng, J. J. Li, R. H. Jin, S. Ye, X. L. Liang and M. Z. Li, “ The development of curved microstrip antenna with defected ground structure” Progress In Electromagnetics Research, PIER 98, 53-73, 2009.

[57] J.-Y. Sze T.-H. Hu and T.-J. Chen, “ Compact Dual-band Annular-ring slot antenna with meandered grounded strip” Progress In Electromagnetics Research, PIER 95, 299-308, 2009

[58] J. Lim, J. Lee, J. Lee, S.-M. Han, and D. Ahn and Y. Jeong, “ A new calculation method for the characteristic impedance of transmission lines with modified ground structures or perturbation” Progress In Electromagnetics Research, Vol. 106, 147-162, 2010.

[59] C. Wu, J. Wang, R. Fralich, and J. Litva, “Analysis of a series-fed aperture coupled patch array antenna”, Microwave and Optical Technology Letters, vol. 4, pp. 110-113, February 1991.

[60] P.K. Singhal, Piyush Moghe.”Design of single layer E-shape Microstrip Patch Antenna”,IEEE,APMC proceeding,2005

[61] Kuchar, Alexander. "Aperture-Coupled Microstrip Patch Antenna Array." Thesis. Technische Universität Wien, 1996.

[62] Manandhar, D. GPS reflected signal analysis using software receiver. Journal of GlobalPositioning Systems, *5*(1–2), 29–34, 2006.